A. Abou-Hassan, V. Cabuil, and O. Sandre

DOI: 10.1002/anie.200904285

Microfluidics

Microfluidics in Inorganic Chemistry

Ali Abou-Hassan, Olivier Sandre, and Valérie Cabuil**

Keywords:
advanced materials · liquid–liquid extraction · microfluidics · microreactors · nanomaterials

Dedicated to Prof. René Massart

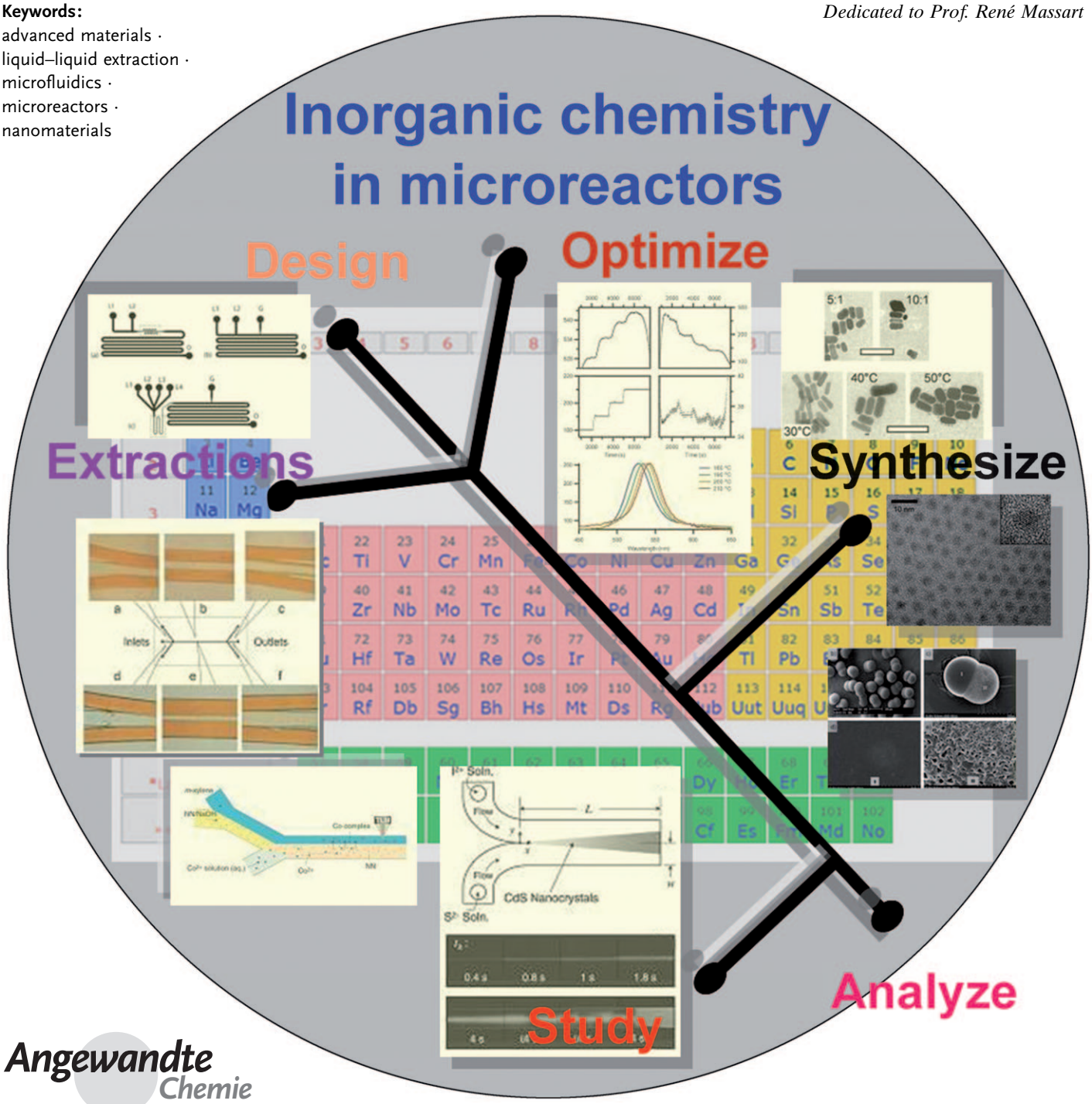

The application of microfluidics in chemistry has gained significant importance in the recent years. Miniaturized chemistry platforms provide controlled fluid transport, rapid chemical reactions, and cost-saving advantages over conventional reactors. The advantages of microfluidics have been clearly established in the field of analytical and bioanalytical sciences and in the field of organic synthesis. It is less true in the field of inorganic chemistry and materials science; however in inorganic chemistry it has mostly been used for the separation and selective extraction of metal ions. Microfluidics has been used in materials science mainly for the improvement of nanoparticle synthesis, namely metal, metal oxide, and semiconductor nanoparticles. Microfluidic devices can also be used for the formulation of more advanced and sophisticated inorganic materials or hybrids.

From the Contents

1. Introduction

Important research efforts in the field of microscale devices have been devoted to analytical sciences to develop miniaturized total analysis systems (μ-TAS).[1–4] The idea behind this concept was to combine classical analytical methods and detection elements that could be placed sequentially to constitute an ideal device that would accomplish all the operations necessary to extract desired information about particular analytes from a complex mixture: sample preparation, chemical conversions, chemical partitions, and signal detection.[1,5,6] Along with the continuing development of μ-TAS and related analytical applications, more and more studies have established the benefits provided by microfluidics to the field of chemistry in general.[7,8] The "lab-on-a-chip" concept emerged to describe a new technology by which each chemical process and system can be miniaturized using microsystem technologies.[9] The key components of a lab-on-a-chip for use in synthetic chemistry are microreactors. These reactors have emerged as a particular class of devices for chemical synthesis and have showed their wide applicability for the optimization of reactions and the production of chemicals.[10–15] To date, the outcome of the reported research has confirmed that microreactor methodology is applicable to both gas- and liquid phase-chemistry.[16,17] The ultimate goal would be to shrink entire chemical and analytical laboratories on a single microstructured chip.[18,19]

The aim of this Review is to provide up-to-date information on microfluidics in the field of inorganic chemistry, and is divided into three major sections. In the first, an overview of available micromixers and microreactors is provided. The following section contains an analysis of the state-of-the-art concerning liquid–liquid extraction of inorganic species using microfluidic devices. The synthesis of several classes of nanoparticles and nanomaterials using some of the unique features that microfluidic reactors offer is then described. Finally, the last section presents some conclusions and future perspectives of this new technology for inorganic chemistry.

2. Microfluidics, Micromixing, and Microreactors

Comprehensive and quantitative reviews of fluid behavior and associated transport processes at the microscale have been presented elsewhere.[20,21] The microreactors are available for chemical applications have also been described in a Review in this journal.[22] This section aims to briefly point out some basic and important aspects of microfluidics and typical micromixers used in chemistry that may be useful to illustrate the Review.

In general, microfluidics can be defined as systems that process or manipulate minute (10^{-9} to 10^{-18} L) amounts of fluids, using channels with dimensions of tens to hundreds of micrometers.[11,23,24] As systems are reduced in size, phenomena such as diffusion, surface tension, and viscosity become ever more important at the micrometer scale.[25] In the case of microfluidic systems with simple geometries, fluid behavior is predominantly influenced by viscosity rather than inertia, resulting in laminar flow. Diffusion can be effective for moving and mixing solutes on the micrometer length scales in laminar flow; however mixing only by diffusion in microfluidic systems can be very slow. To overcome this limitation and improve the mixing of fluids, a wide range of systems have been designed.[14,26,27] These devices are based on the principle

[*] Dr. A. Abou-Hassan, Dr. O. Sandre, Prof. V. Cabuil
UPMC Univ Paris 06, UMR 7195 PECSA, Physicochimie des Electrolytes, Colloïdes, Sciences Analytiques
75005 Paris (France)
and
CNRS, UMR 7195 PECSA, Physicochimie des Electrolytes, Colloïdes, Sciences Analytiques
75005 Paris (France)
and
ESPCI, UMR 7195 PECSA, Physicochimie des Electrolytes, Colloïdes, Sciences Analytiques
75005 Paris (France)
E-mail: ali.abou_hassan@upmc.fr
valerie.cabuil@upmc.fr
Homepage: http://www.pecsa.upmc.fr

that the liquid stream has to be split into a multitude of smaller streams before making them combine. This increases the surface area of interaction between the two fluids that have to be mixed and consequently speeds up the mixing process.[28]

Micromixers are usually categorized as being passive or active. Passive micromixers do not require external energy; the mixing process relies entirely on diffusion or chaotic advection, whereas active mixers rely on time-dependent perturbations of the fluid flow to achieve mixing.[14,29–35] Figure 1 shows the laminar and the droplet-based micromixers that will be often encountered in this Review as microreactors for liquid–liquid extraction or for nanoparticle synthesis. The interested reader can refer to the reviews of Nguyen and Wu[26] and Hessel et al.[36] for detailed accounts on micromixing.

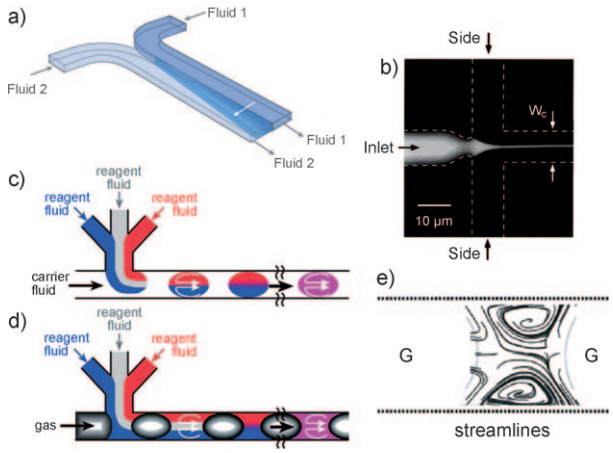

Figure 1. Some examples of different passive mixing techniques used in chemical synthesis. a) Mixing of two miscible fluid streams by flow lamination. The component streams mix only by diffusion, creating a dynamic diffusive interface with predictable geometry. Reproduced from Ref. [25], copyright Elsevier Science B.V., 2005. b) By hydrodynamic focusing of the inner stream (inlet) by an outer stream (side). Reproduced from Ref. [30], Copyright the American Physical Society, 1998. c) Encapsulated mixing in discrete liquid plugs. d) Liquid slugs. Reproduced from Ref. [47]. e) Recirculation streamlines in a gas–liquid segmented flow. Reproduced from Ref. [32], copyright the American Chemical Society 2005.

Because of their small dimensions, micromixers offer several advantages for the chemical processing.[37] Process parameters such as pressure, temperature, residence time, and flow rate can be easily controlled.[10] The hydrodynamic flow in the microchannels is essentially laminar, directed, and highly symmetric compared to macroscale conduits in which flow regimes are always turbulent.[38] Mixing times in micromixers are smaller than in conventional systems and, owing to the small dimensions, the diffusion times are very short, enabling the control and rapid creation of a homogeneous reactant mixture.[14,39] Moreover, because of their high surface-to-volume ratio, microfluidic reactors can afford a high heat -exchanging efficiency compared to that of traditional heat exchangers, allowing the reaction mixture to be heated or cooled within the microstructure rapidly and work under isothermal conditions with exactly defined residence times.[10,37,40] The small reactor volumes (nL–μL) result in minimal reagent consumption and fast responses to system perturbations, allowing a rapid adjustment of the experimental conditions to tune the material properties in real time.[41] Integration of chemical detection in the microfluidic system would enable high-throughput screening of the chemical process under controlled conditions, which is often difficult in conventional macroscopic systems.[39] Microstructured reactors offer also many opportunities for new production concepts by offering possibilities to perform large numbers of independent chemical reactions for the purpose of synthesizing new compounds.[39,42] Multiple process steps and/or parallel reactions can be integrated on a single chip with microfabricated networks having individually addressable microchannels and reservoirs.[43,44] Continuous synthesis is believed to be one advantage of microreactor technology, which means the possibility of running up to 24 h per day and carrying out analyses on-line.[45] In particular, a multistep continuous synthesis in a microreactor is expected to provide better quality functional products with improved economics for complicated reactions.[8] In a continuous-flow system, reactions are performed at steady-state, making it possible to achieve better control and reproducibility.[46] Furthermore, the ability to manipulate reagent concentrations in both space and time within the channel network of a microreactor provides an additional level of reaction control that is not attainable in bulk stirred reactors where concentrations are generally uniform. Furthermore, the spatial and temporal

Ali Abou-Hassan was born in Lebanon. He received his BSc and MSc degrees in chemistry from the Pierre & Marie Curie University (UPMC, Paris 6). He completed his PhD work on using single-phase flow microfluidics to study the synthesis and the functionalization of magnetic nanoparticles at the PECSA Lab at the Pierre & Marie Curie University under the direction of Prof. V. Cabuil. Abou-Hassan is currently undertaking postdoctoral research at the Max Planck Institute for Colloids and Interfaces, where he is working on the self-assembly of inorganic nanoparticles under the direction of Prof. H. Möhwald.

Olivier Sandre graduated from the ESPCI Paris School of Physics and Chemistry in 1996. He received his PhD in 2000 from UPMC Paris 6 University at the Physicochimie Curie lab under the supervision of Prof. F. Brochard-Wyart. In 2001, he spent a post-doctoral year at UC Santa Barbara before starting his career as CNRS researcher in the group of Prof. V. Cabuil at UPMC Paris 6 to elaborate new nanocomposite materials based on polymers and magnetic nanoparticles.

control of chemical reactions in microreactors, coupled with the features of very small reaction volumes and high surface interactions, can be useful to control and alter chemical reactivity relative to the situation of homogeneous solutions in a rapid and efficient manner.[7–47]

3. Microfluidics for Liquid–Liquid Extraction of Inorganic Species

Separation is an important problem in chemical engineering; even though it involves organic solvents, liquid–liquid extraction (LLE) remains one of the most efficient techniques to selectively extract or separate neutral organic or inorganic species. Inorganic chemistry is mostly concerned with LLE, for example when heavy metals have to be removed from effluents, or when actinides or long-lived radionuclides have to be separated.[48] Usually metallic species are extracted from water into organic solvents after chelation or formation of ion pairs. Curiously, even if LLE is widely used and mastered, the transport of molecular or ionic species from one phase to another through an interface is still not fully understood. The area of the interface is of course a key parameter. As microfluidics allows a major increase in the surface-area-to-volume ratio, it is of utmost importance to consider the use of microchips to improve or study the separation and extraction processes. This concept has been widely investigated by Kitamori and co-workers, who proposed a general methodology for the integration of all the usual unit operations of chemical engineering onto a microchip.[45,49] He was the first to use glass microchips for studying molecular transport, namely the extraction of a nickel dimethylglyoxime complex from water into a chloroform phase.[50] The chelates in organic solvent were quantified using the thermal lens microscope (TLM) developed in his lab, which allows even non-fluorescent molecules to be localized.[51] When fluorescent complexes are extracted, for example Al-DHAB (DHAB = 2,2 dihydroxyazobenzene) into the organic phase, spatially resolved fluorescence spectroscopy can be used to study the extraction. The concentration of Al-DHAB in the oil phase was thus mapped in the microchannel during extraction by 2,2-dihydroxyazobenzene and compared to simulations.[52]

Kitamori showed that extraction was possible in a microchannel, and found that for the extraction of an iron(II) complex by a chloroform solution of 1-octanaminium-*N*-methyl-*N*,*N*-dioctyl chloride (Figure 2), an extraction time of about 45 s was determined, which is about 20 times shorter than the extraction time in bulk using mechanical shaking.[53] By coupling micro-unit operations (MUOs),[45,49] he could successfully carry out the synthesis of a complex (chelation of Co^{II} by 2-nitroso-1-naphtol) and its extraction (into *m*-xylene) in the same chip.[54]

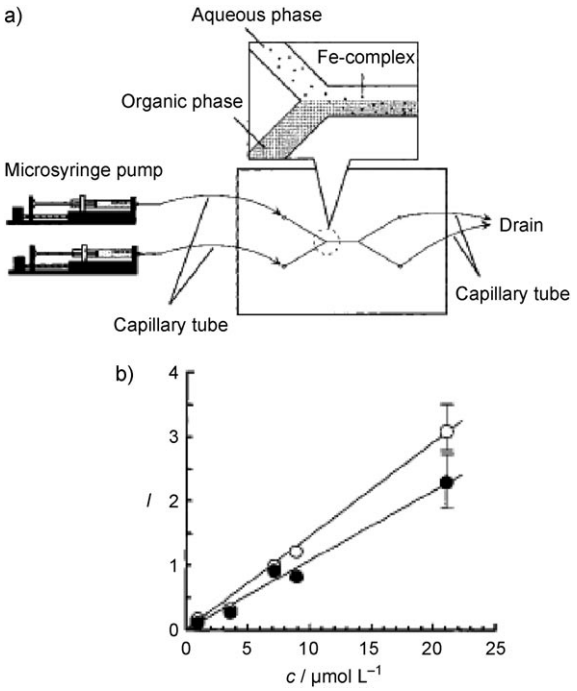

Figure 2. a) Diagram showing the integrated microextraction system. b) Dependence of the thermal lens microscope signal intensity on the concentration of iron(II) solution introduced: ● microchannel, ○ separatory funnel. Reproduced from Ref. [53], copyright American Chemical Society 2000.

To stabilize the interface, the length of the extraction zone was shortened and the angle made by the two liquid streams was reduced.[55] Another improvement was provided by fabricating intermittent partition walls at the center of the separation microchannel to successfully extract yttrium ions by 2-ethylhexylphosphonic acid mono-2-ethylhexyl ester from an aqueous acidic mixture of yttrium(III) and zinc(II) ions. Flow analysis and modeling revealed that the partition induces a slight turbulence that promoted the extraction.[56] As the area of the interface is a key parameter for LLE, several methods to induce an increase of this area have been proposed. One solution is to produce stable multilayer flows in microchannels, as proposed by Hibara et al.[57] This kind of chip was used to extract an aqueous Co-DMPA complex (DMPA = dimethylaminophenol) into *m*-xylene. The *m*-xylene was sandwiched in the central channel between the diluted aqueous solutions of cobalt complex (5–10 mol L^{-1}). The concentration of the complex in the *m*-xylene phase was measured using Kitamori's TLM. The extraction process in this three-layer flow system attained equilibrium about 3 s

Valérie Cabuil has been a full professor at Pierre & Marie Curie University (Paris 6) since 2001. She is director of a laboratory involved in colloidal science and physical chemistry (PECSA Lab) and of a doctoral school devoted to physical and analytical sciences. Her research deals with (magnetic) inorganic nanoparticles, their synthesis, modification, and colloidal stability. She recently introduced microfluidics into her laboratories for the synthesis and modification of inorganic nanoparticles.

after the contact, which has to be compared to the 60 s found in a diphasic configuration. Such a three-layer flow system was also used for the selective extraction of yttrium by 2-ethylhexylphosphonic acid mono-2-ethylhexyl ester as a liquid membrane separation system: The organic phase containing the extracting agent was sandwiched between the feed aqueous phase (an Y^{3+}/Zn^{2+} aqueous acidic mixture) and the receiving aqueous phase (a 1M nitric acid solution). Y^{3+} ions selectively permeated through the liquid membrane within several seconds.[58]

To extract different ions from an aqueous mixture on the same chip, sequential pumping of different organic phases, each one of them containing an extracting agent specific to the ions to extract, was performed.[59] The concept was tested with the extraction of sodium and potassium ions and appeared to be efficient.

More recently, droplet-based microfluidics was proposed to optimize liquid–liquid extraction (Figure 3).[60] The idea was again to extend the interface area, the latter being independent of the channel geometry but easily controlled through the droplet size. Extraction of Al-DHAB complex from water to TBP (tributyl phosphate) was performed in a T-shaped microchannel, with the Al-DHAB complex introduced as the continuous phase and TBP as the dispersed phase. The efficiency of extraction was estimated from fluorescence measurements at several points of the channel. Again, extraction times (about 1 s) appeared to be about 90 times shorter than times found for conventional methods. For the same specific interface area, extraction efficiency was not better in this configuration than in conventional devices; nevertheless, large mass-transfer coefficients were obtained using such a droplet-based microfluidic system compared to conventional mechanical shaking. A chip-based sequential-injection droplet array liquid–liquid extraction system was proposed more recently with chemiluminescence as an alternative to fluorescence for the detection of the extracted species.[61]

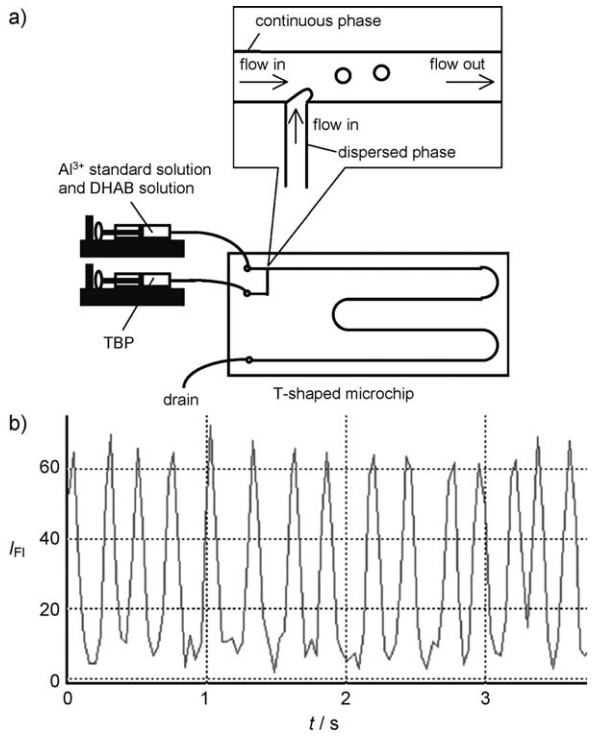

Figure 3. a) Droplet generation in a T-shaped microchip. b) Fluorescence signal of Al^{3+}-DHAB in each droplet obtained at a distance $x = 53$ mm from the confluent point. Flow rate of the continuous phase: 37 mm s^{-1}; flow rate of dispersed phase: 25 mm s^{-1}. The concentration of the Al^{3+} solution was 80 μg L^{-1}. DHAB = 2,2-dihydroxyazobenzene. Reproduced from Ref. [60], copyright Elsevier B.V. 2006.

To summarize, it appears that in all cases, microreactors (continuous-flow or droplet-based) accelerate separation and allow strategies to control selectivity for the extraction of inorganic cations. Results are less clear concerning enrichment factors (abundance of a chemical element in one phase compared to another one), which are not often explicitly discussed. As a fundamental point, microreactors can be used as convenient tools to investigate separation phenomena, explore selectivity of extractants, and screen their efficiency as soon as spectroscopic techniques that allow a local characterization of the species in the channel are available.

4. Microfluidics for the Synthesis of Inorganic Materials

In the following section, we shall focus on the synthesis of inorganic nanoparticles in microfluidic devices. Indeed, it is the topic that has been most considered in the field of inorganic synthesis in recent years. The main questions addressed relate to the control of the size and shape of the nanoparticles, and microfluidics has been considered as a possible technology to allow the investigation and the control of nanoparticle synthesis.

We first briefly recall the process of particle formation as explained by the classical nucleation theory (CNT), which occurs in the absence of a solid interface and consists of combining solute molecules to produce nuclei.[62] Three steps are usually considered: nucleation, growth (primary growth), and aging (secondary growth). In the nucleation step, tiny particles precipitate spontaneously from a supersaturated precursor solution. When the precursor concentration falls below the minimum concentration for nucleation, the latter stops, but growth continues. Crystal growth occurs by addition of soluble species on the solid phase. In most cases, nucleation and growth occur concurrently throughout particle formation, and the final particles therefore exhibit a broad size distribution. Apart from these points, the size of the critical nuclei and the particle growth rate depend on the experimental conditions (concentration, temperature, and pressure). Thus, to achieve a narrow size distribution, a short nucleation period (that generates all of the future particles) followed by a self-sharpening growth process and a constant chemical environment are required. Microreactors can be designed to meet these requirements, and a large number of microreactors have been reported for nanoparticle synthesis.

Three families of inorganic materials have been mainly studied: metals, metallic oxides, and semiconductors. We shall begin this section by a short review of all the microreactors

that have been used for the synthesis of inorganic nanoparticles. Then each kind of materials under consideration will be detailed, and finally composite materials based on inorganic nanoparticles that have been obtained thanks to microfluidics will be described.

4.1. Microreactors for Synthesis

Microfluidic reactors fabricated to date are made of glass, silicon, poly(dimethylsiloxane) (PDMS), stainless steel, ceramics, or the commonly used epoxy-based negative photoresist SU-8.[28,63–66] Glass is still a favorite material for the chemist, who is familiar with its chemical robustness and optical transparency. Silicon also has much to offer because of its electrical properties and compatibility with a multitude of fabrication processes, including the integration of electrical circuits. Depending on the final use and application, the materials with the best advantages are chosen: If high-temperature reactions (>200 °C) are carried out, glass-based microreactors are preferred. For applications at room temperature or up to 200 °C, polymer-based microreactors can be used, except if organic solvents are needed, as is the case for liquid–liquid extraction. In such cases, glass is again preferred.

Both single-phase continuous-flow microreactors and emulsion (two-phase) microdroplet/segmented-flow microreactors have been reported for the elaboration of nanomaterials. Continuous-flow reactors have been widely used for synthesis owing to their simplicity and operational flexibility.[67] Reagents mix and react under diffusion-based laminar flow; reaction times, temperatures, mixing efficiency, and reagent concentrations are the typical control parameters for the synthesis of nanomaterials.[68] A significant problem encountered in single-phase microfluidic systems is that of achieving rapid and efficient mixing of the fluids whilst minimizing the Taylor–Aris dispersion effect caused by the parabolic (Poiseuille) velocity profile (Figure 4a).[69] The latter is responsible for the large distribution of residence times that may cause significant variation in the yield, efficiency, and product distribution of a reaction.[14] The confinement of reactions in nanoliter-sized droplets can serve as a method to overcome this problem.[47] In multiphase microfluidic reactors, reactants are compartmented into droplets or "plugs" effectively narrowing the residence time distribution in both phases (Figure 4b).[31,34] In one common multiphase system, the continuous phase is oil, which totally wets the walls of the microfluidic channel, and the droplets are made of the aqueous synthesis mixture.[31] In the case of gas–liquid reactions or reactions in anhydrous solvents, gas–liquid segmented reactors have also been developed: In such reactors, the droplet phase consists of discrete bubbles of a gas within a liquid continuous phase.[32] Such reactors can be convenient for kinetic studies; for example, Laval et al. recently developed a droplet-based microfluidic system that allows the droplets to be stored on-chip and to control precisely their temperature in such a small volume.[70] It was possible to quantify the nucleation rate of KNO_3 precipitation in water by direct measurements; the precipitation seems to occur through heterogeneous mechanisms that involve impurities with different activities randomly distributed among the droplets up to supersaturation S close to $S = \ln(c/c_{sat}) \approx 8$.

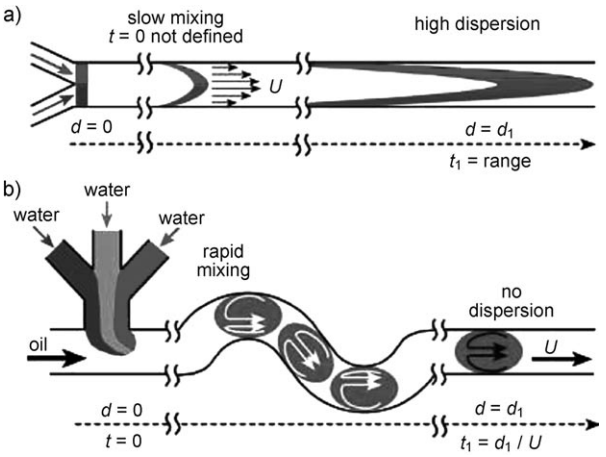

Figure 4. Comparison of a reaction A + B conducted in a) a standard pressure-driven microfluidic system device (reaction time $t \neq d/U$), and b) in a droplet-based microfluidic system (reaction time $t = d/U$). Two aqueous reagents (red: A, blue: B) can form laminar streams separated by a partitioning aqueous stream in a microchannel (gray). When the three streams enter the channel with a flowing immiscible fluid, they form droplets (plugs). The reagents come into contact as the contents of the droplets are rapidly mixed. Internal recirculation within plugs flowing through channels of different geometries is shown schematically by arrows. Reproduced from Ref. [31].

4.2. Synthesis of Semiconductors

Semiconductor nanoparticles, that is, quantum dots (QDs) formed of binary compounds such as CdS, CdSe, and ZnS, were the first nanoparticles synthesized in a microfluidic device.[71] They are of considerable scientific and commercial interest owing to their tunable optical and electronic properties and potential applications in a wide range of electronic devices.[72] Physical properties of these nanocrystallites are strongly related to their physical size and shape. Indeed, there is considerable interest in processing routes producing nanoparticles of well-defined size.[73] The most successful and widely adopted QD synthesis involves the injection of a liquid precursor into a hot bulk liquid, followed by growth at a lower temperature in the presence of stabilizing surfactants.[74] Controlling the conditions of such a process in bulk is difficult,[75] and microfluidics has thus been proposed as an alternative synthetic approach to control nanocrystal growth.[76] Indeed, the direct correlation between the diameter of QDs and the UV/Vis absorption allows a rapid on-line particle size determination.[46,76]

Microfluidic synthesis of CdS nanoparticles after mixing of $CdNO_3$ and Na_2S (in the presence of a sodium polyphosphate stabilizer) in a laminar microfabricated mixer[77] was first reported by Edel et al. in 2002.[71] A broad range of crystallite sizes with an improved monodispersity (compared to bulk synthesis) was obtained by increasing the residence time of the reagents.

As laminar reactors are subjected to Taylor dispersion and clogging, Shestopalov et al.[78] isolated the reaction inside aqueous droplets, which were surrounded and transported by a fluorocarbon oil immiscible with water (Figure 5). Aqueous

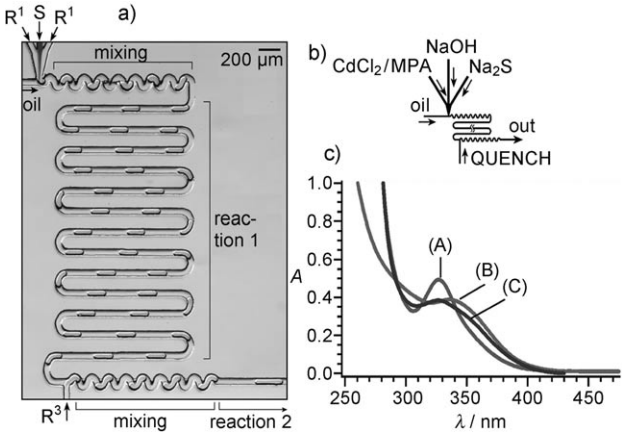

Figure 5. a) Micrograph of a PDMS microfluidic device used to perform droplet-based synthesis of nanoparticles; R^{1-3} = reagents, S = partitioning stream. b) Two-step synthesis on chip with millisecond quenching yields CdS colloidal nanoparticles that are less disperse than those synthesized on chip. c) UV/Vis spectra of nanoparticles synthesized on chip with millisecond quench (A), on a chip without quenching (B), and on the benchtop (C). Reproduced from Ref. [78], copyright Royal Society of Chemistry 2004.

droplets containing $CdCl_2$, mercaptopropionic acid (MPA), Na_2S, and NaOH solution were formed within 5 ms in the oil flow. The control of the CdS particles (and of core/shell CdS/CdSe nanostructures) was improved when the microreactor was used. Later on, to reduce technical problems, increase the mixing time, and lower the dispersion effect, Hung et al. proposed a microfluidic device that can alternately generate droplets and fuse them under a velocity gradient in an expansion chamber (Figure 6).[79]

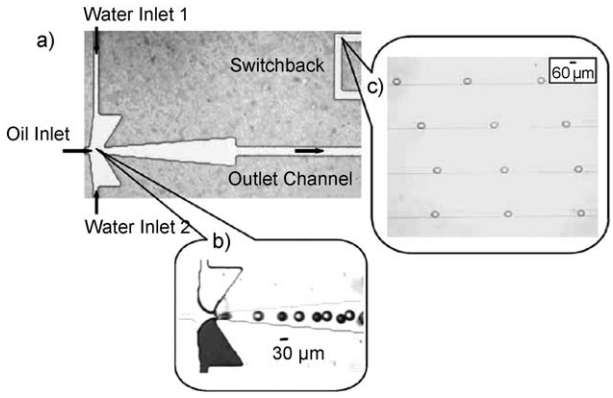

Figure 6. a) Microscope image of the PDMS channel magnified at the doublet T-junction channel. b) Water-in-oil alternating microdroplet generation; colored dye is added into water inlet 2 for the differentiation purpose. c) Fused droplets align in the long switchback channel. Reproduced from Ref. [79], copyright Royal Society of Chemistry 2006.

Fundamental investigations into the reaction process was reported by Sounart et al., who synthesized cysteine-stabilized CdS nanoparticles in a continuous-flow microfluidic reactor and studied the particle growth in situ by spatially resolved photoluminescence imaging and spectroscopy.[80] Their results provided a direct insight into the kinetics and the mechanistic data of the QD formation.

CdSe nanoparticle synthesis has also been extensively studied.[32,46,76,81–84] In initial experiments described by Nakamura et al., CdSe QD synthesis was performed continuously within a fused silica capillary (200–500 µm id (inner diameter)) immersed in an oil bath at temperatures ranging from 230 to 300 °C and with reaction residence times determined by the volumetric rates and the capillary dimensions.[81] Large nanoparticles were obtained by increasing the temperature or the residence time. To minimize the distribution of the residence times generated by hydrodynamic pumping of fluids through the microchannel, the authors segmented the reaction solution with nitrogen bubbles at defined intervals.

A more detailed study of size-controlled growth of CdSe nanoparticles in microfluidic reactor has been reported by Chan et al.[76] A heated microfabricated borosilicate glass chip-based reactor was used for the continuous high-temperature synthesis, control, and characterization of CdSe nanocrystals. Dimethylcadmium was mixed with selenium dissolved in boiling trioctylphosphine oxide (TOPO) and octadecene (ODE) in the microfluidic reactors, and the effect of the temperature, flow rate, and concentration of precursor in solution was studied, whereby all of these parameters were varied independently. For example, increasing the temperature resulted in an increase of the particle size and a narrowing of the size distribution.

Outgassing and clogging are usual problems encountered during the synthesis within microreactors at high temperatures. Yen et al.[46] avoided these problems by using appropriate chemical reagents. Cadmium oleate and TOP-Se complexes were dissolved in a high-boiling-point solvent system consisting of squalane, oleyl amine, and TOP. The synthesis was carried using a continuous-flow reactor with a miniature convective mixer followed by a heated glass reaction channel maintained at a constant temperature (180–320 °C). The authors elegantly showed the possibility of fine-tuning the size of CdSe nanocrystals produced in the reactor by systematically varying the temperature, flow rate, and concentrations. Later, the same group reported the use of a gas–liquid segmented-flow reactor with multiple temperature zones for the synthesis of high quality CdSe quantum dots.[32] The reactor design allows rapid mixing of the precursors and on-chip quenching of the reaction. The authors compared their results to those obtained in the continuous-flow method and concluded that the enhanced mixing and narrow residence time distribution characteristic of the segmented-flow reactor resulted in a significant improvement of the reaction yield and of the size distribution, especially for short reaction times during the synthesis of CdSe nanoparticles.

Synthesis of CdSe nanoparticles at high pressures and temperatures in a continuous microfluidic reactor was recently reported by Marre and co-workers.[84] They carried

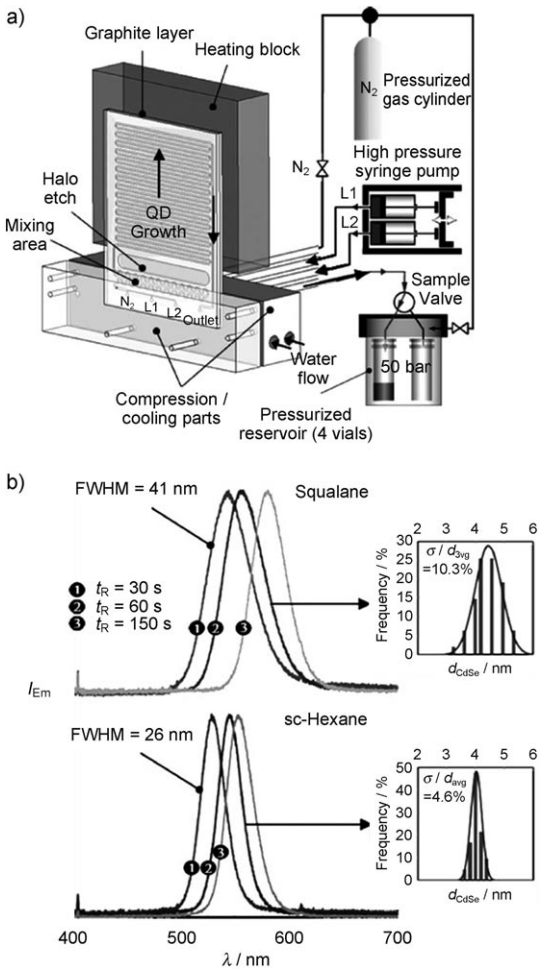

Figure 7. a) The experimental set-up used for the synthesis of QDs. The microreactor consists of a 400 μm wide and 250 μm deep channel with a 0.1 m long mixing zone maintained at room temperature and a 1 m long reaction zone heated up to 350 °C. The entire set-up was first pressurized from the inlet to the outlet using a nitrogen gas cylinder. Thereafter, the nitrogen valve was closed and the two precursor solutions (L1,2) were delivered independently using a high pressure syringe pump, insuring good control of the flow rate. b) Photoluminescence spectra at different residence times (t_R) obtained for CdSe QDs synthesized in squalane and supercritical (sc) hexane at 270 °C, 5 MPa with $[Cd] = [Se] = 3.8 \times 10^{-3}$ M and the QD size distribution obtained from TEM measurements for samples run at $t_R = 60$ s; FWHM = full width at half maximum. Reproduced from Ref. [84].

out the synthesis using either squalane or supercritical hexane as a solvent (Figure 7). The synthesis in hexane (liquid or supercritical) resulted in a decrease of 2% in the size distribution of the QDs due to a decrease of the residence time distribution caused by its lower viscosity compared to squalane. Most notably, the use of supercritical hexane led to higher supersaturation compared to squalane, producing a larger number of nuclei, thus narrowing the size distribution of QDs.

Temperature gradients can be also used to induce a better control over the nucleation and growth of the nanoparticles and narrow the size distribution. Steep temperature gradients were created in a heating section of a microreactor designed to induce burst nucleation of CdSe in its high-temperature zone and to promote growth in its low-temperature zone (Figure 8).[85] The superiority of this two-temperature approach on the kinetic control of the QDs could be demonstrated, as the synthesized nanoparticles had a higher nuclei concentration and narrower size distribution.

Synthesis of doped semiconductor nanoparticles in microfluidic devices has also been reported. Singh et al. investigated the synthesis of 1-thioglycerol-capped manganese-doped ZnS semiconductor nanocrystals by a microfluidic approach at room temperature and at 80 °C.[86] Photoluminescence, X-ray photoelectron spectroscopy, atomic absorption spectroscopy, and electron paramagnetic resonance studies confirmed the presence of Mn^{2+} in the ZnS nanoparticles.

The stability and properties of QDs are improved by coating the semiconductor cores (CdS, CdSe) by a nanometric shell (or even two) of another semiconductor as ZnS.[87] The thickness of the ZnS shell is crucial to obtain high quantum

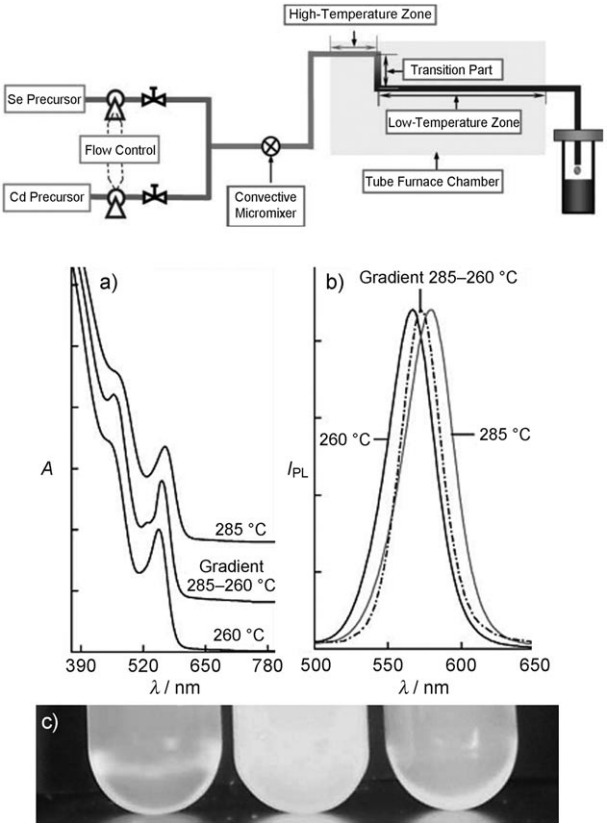

Figure 8. Top: Process map for the synthesis of CdSe QDs in a capillary microreactor with a two-temperature approach in the heating section. The microreactor consists of a convective mixer placed before a capillary tube (300 μm id). The latter was formed of three different parts, the lengths of which can be varied: 1) a high-temperature zone to induce burst nucleation, 2) a transition zone, and 3) a low-temperature zone to promote growth of the nanoparticles. Bottom: a) Absorption spectra and b) photoluminescence spectra of the samples produced using the two-temperature approach and the constant temperature approach for the microreaction with the same residence time; c) emission from the three samples with the same absorption value at 365 nm under 365 nm UV light (from left to right: 260 °C, 285–260 °C, 285 °C). Reproduced from Ref. [85], copyright Royal Society of Chemistry 2008.

yields of the ZnS-capped CdSe Qds,[88,89] and microfluidics appears very promising in performing such a controlled coating. Wang et al. reported the first multistep continuous-flow method for the synthesis of ZnS-coated CdSe QDs using microfluidic reactors.[90] UV/Vis spectra showed that CdSe particles and the ZnS coating were produced consecutively. The particle size and the layer thickness were directly adjusted by the flow rate. In another work, the same authors focused their study on the optimization of the coating step, by using in the same microreactor as the one described above and a single molecular source, $[\{(C_2H_5)_2NCSS\}_2Zn]$, that has a low toxicity and a good stability in air.[91] The effects of the residence time, the CdSe core size, and the temperature on the final coating and on the photoluminescence quantum yield were investigated by absorption and photoluminescence spectroscopy. Fluorescence quantum yields above 50% were obtained when an optimized residence time was chosen in the microreactor. Quantum yields remained high even when the nanocrystal surface was modified to be hydrophilic. Recently, a facile method based on microfluidic for the synthesis of CdSe/ZnS core/shell structures with pure green luminescence involving short residence time and low reaction temperature ($t = 10$ s, $T = 120$ °C) was developed by Luan et al.[92] CdSe nanoparticles and Zn sources were mixed by a convective mixer before entering a heated PTFE capillary for the coating process. As the temperature for the coating step was low, the synthesis of the core/shell nanoparticles was continuous and did not require any purification of the CdSe nanoparticles. Homogeneous coatings of ZnS were achieved with fairly wide operation parameters, such as residence times and temperatures. The synthesis of ZnS/CdSe/ZnS particles using microfluidic reaction technology was also explored.[93] Thanks to the homogeneous and accurate control of heating temperature and time in a microreactor, the true epitaxial deposition of CdSe monolayers onto the ZnS nanocrystals was possible, despite the lattice mismatch between ZnS and CdSe. The fluorescence wavelength and the quantum yield of these nanoparticles were tuned by controlling the flow rate during the CdSe layer deposition step.

4.3. Synthesis of Oxide Nanoparticles

Oxide nanoparticles are widely used and described. They can be obtained through several procedures, some of them being easily transposable into microfluidic devices.[44,94–101]

Wang et al. obtained TiO_2 nanoparticles from the hydrolysis and condensation of titanium tetraisopropoxide (TTIP) at room temperature using the stable interface obtained with the appropriate flow rates and viscosity ratios between two immiscible laminar flows in a microchannel reactor.[94] The authors described the water/oil interface as a novel type of nano-like reaction chamber and expected special characteristics to be obtained assuming that the particle growth mechanism at the interface of immiscible flows may be different from that in beakers. TiO_2 colloids were collected at the outlet of the microreactor and characterized off-line using UV/Vis spectra and TEM images, which confirmed the presence of the TiO_2 anatase polymorph. Based on the same idea of conducting reactions at the interface of two immiscible liquids and to avoid the precipitation of the particles at the walls, Takagi et al. developed a microreactor with double-pipe structure.[95] Two immiscible liquids were allowed to flow, one in the inner and one in the outer tube and maintained an annular and laminar flow of two separated phases that create a microspace delimited by the outer fluid wall. The inner flow acted as a microchannel, the radius of which can be varied by the operating conditions. The particles thus produced at room temperature were spherical particles of amorphous titania with a monomodal, narrow size distribution compared to the random size distribution obtained in a conventional batch method. It was also possible to control the particle size in the range from 40 to 150 nm simply by changing the diameter of the inner tube at a low TTIP concentrations.

Khan et al. studied the influence of reactor design and the parameters of linear flow velocity and the mean residence times on SiO_2 particle size distribution.[98] The particles were obtained using the so-called Stöber process.[102] Two reactor configurations were examined: laminar-flow reactors and segmented-flow reactors (Figure 9). As laminar-flow reactors are affected by axial dispersion at high linear velocities, wide size distributions of colloidal SiO_2 were observed. In segmented-flow reactors, the internal backflows created inside the liquid plugs generated mixing, which eliminated the axial dispersion effects and produced a narrow size distribution of silica nanoparticles.

Ferric oxides have also been synthesized in microreactors (Figure 10). Decomposition of $Fe(NO_3)_3$ in formamide at 150 °C was performed in microreactors consisting of capillary tubes of the same or different inner diameters made of glass, treated with trimethylsilyl (TMS) chloride and polyimide, and then immersed in an oil bath maintained at 150 °C.[101] A conventional autoclave was also used for comparison. Haematite nanoparticles, α-Fe_2O_3, with different shapes were obtained depending on the microreactor. A comparison of the surface area of the reactor normalized by the reactor volume indicated an acceleration of the reaction when the specific area was increased.

The continuous microsynthesis of stable magnetite nanoparticles Fe_3O_4 by co-precipitation of an aqueous solution of a stoichiometric mixture of iron (II) and iron(III) salts by an alkaline medium was reported by our group.[99] The reactor consisted of the same coaxial-flow microreactor as the one reported by Takagi et al. for the synthesis of TiO_2 nanoparticles.[95] The outer capillary was obtained by molding in PDMS (1.6 mm id) and the inner capillary was of glass (150 μm id). The flow rates of the miscible liquids were continuously varied to achieve fast mixing and different residence times. At the outlet of the reactor, the reaction was quenched by solvent extraction in cyclohexane using a surfactant. The superparamagnetic behavior of the nanoparticles and their spinel structure were confirmed by vibrating sample magnetometry (VSM) and electron diffraction, respectively. From the VSM measurements, it was concluded that the nanoparticles produced within a few seconds in the channel presented a narrow size distribution below the typical values obtained by the batch co-precipita-

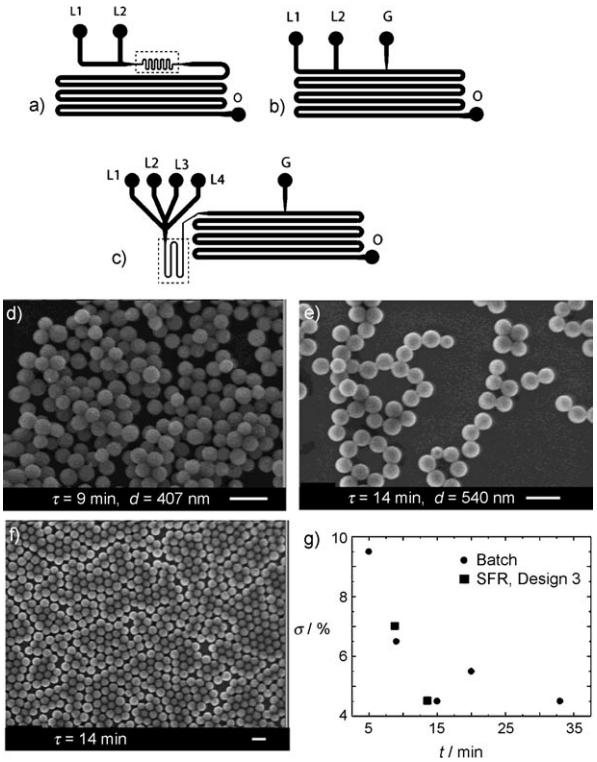

Figure 9. Schematic diagrams of microfluidic channels: a) Design 1 (laminar-flow reactor, LFR) has two liquid inlets (L1 and L2) and one outlet (O). b) Design 2 (segmented-flow reactor, SFR) has two liquid inlets (L1 and L2), a gas inlet (G), and an outlet (O). c) Design 3 (SFR) has four liquid inlets (L1–L4), a gas inlet (G), and an outlet (O). d–f) Sequence of SEM micrographs corresponding to various residence times: d) 9 min; e) 14 min, f) low magnification SEM of sample (e); the organization of particles into pseudocrystalline domains is an indicator of the high monodispersity of the microreactor product. g) Graph of standard deviation σ expressed as a percentage of mean diameter versus residence time t in the SFR as compared to batch reactor data. In all SEM micrographs, the scale bar corresponds to 1 μm. Reproduced from Ref. [98], copyright American Chemical Society 2004.

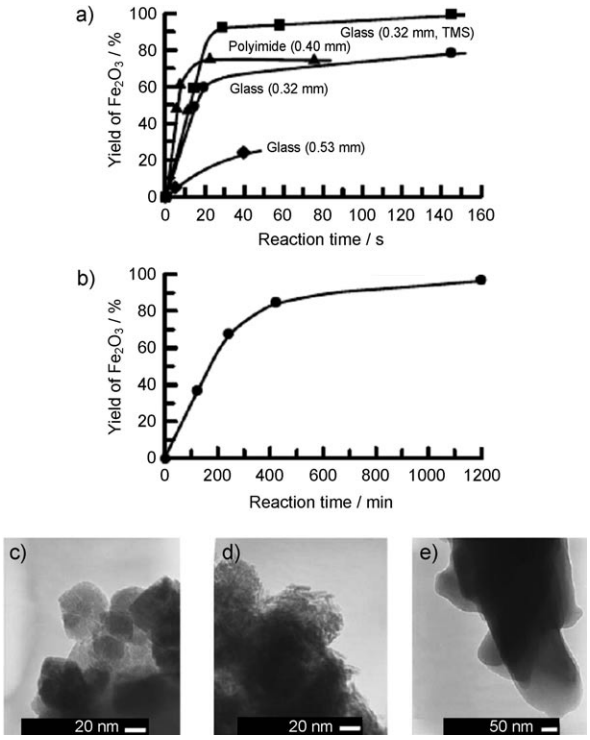

Figure 10. Influence of the reaction time on the yield of α-Fe_2O_3; a) capillary tube reactors, b) autoclave (50 mL). TEM images of the products: c) glass capillary, d) glass capillary with TMS (trimethylsilyl chloride)), and e) autoclave (50 mL). Reproduced from Ref. [101], copyright Springer 2005.

tion and exhibited a small decrease of ordering of their magnetic moments.[103] Later on, the same setup was improved by separating a nucleation reactor and an aging channel to synthesize antiferromagnetic ferrihydrite α-FeOOH nanoloths.[44] In the nucleation microreactor, ferrihydrite nanoparticles were precipitated by fast mixing of $FeCl_3$ and an alkaline solution of tetramethylammonium hydroxide (TMAOH). The suspended ferrihydrite nanoparticles were directly injected from the outlet into a microtubular aging coil (1.7 mm id) continuously heated in a water bath at 60 °C. TEM and HRTEM images confirmed the acceleration in the aging process of the ferrihydrite phase into goethite: plate-like nanostructures of goethite were detected after only 15 min of continuous aging in the microreactor, whereas several hours are necessary in batch conditions. A droplet-based synthesis of magnetic iron oxide nanoparticles was also reported by Frenz et al.[100] The authors designed a microfluidic reactor that enabled droplet pairs to be generated based on hydrodynamic coupling of two spatially separated nozzles (Figure 11). One of the droplets contained the Fe^{2+}/Fe^{3+} mixture whilst the other contained the ammonium hydroxide solution. When an electrical field was applied between the two on-chip electrodes, the droplet pairs coalesced and a precipitate of iron oxide nanoparticles appeared. Nanoparticle size measurements by TEM showed that the average particle diameter was smaller for the fast microfluidic compound mixing (4 ± 1 nm) than for bulk mixing (9 ± 3 nm). The absence of hysteresis in the magnetization curve and the high resolution TEM images confirmed the iron oxide spinel structure.

As it was the case for quantum dots, core/shell oxide nanoparticles have also been synthesized in microfluidic devices. Khan et al. developed, for the coating of colloidal SiO_2 by TiO_2, a continuous-flow microreactor allowing a controlled multipoint addition and mixing of a reactant to a primary feed (Figure 12).[104] The segmented gas–liquid-flow coating device enabled the multistep addition through a branched manifold and the rapid mixing of small amounts of titanium tetraethoxide (TEOT) throughout the process, yielding coatings of controlled thickness. When the TEOT was added in a single step to a relatively monodisperse silica particle suspension, a polydisperse mixture of primary coated particles, secondary titania particles, and large agglomerates were observed. In contrast, when the branched manifold was used to feed the TEOT solution, the monodisperse nature of the initial particles population was preserved and both the secondary particle formation and agglomeration were avoided. After calcination at 500 °C, the core/shell nature of

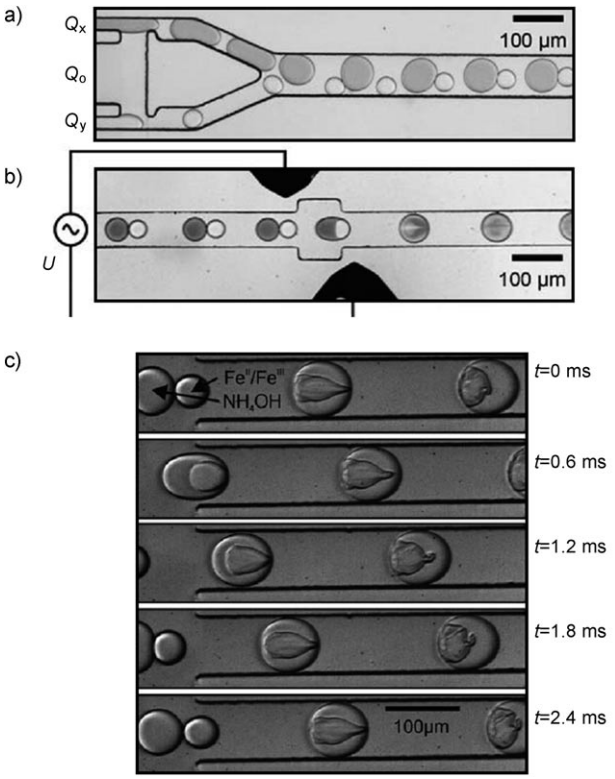

Figure 11. a) Pairing module. Two aqueous phases are injected by the outer channels and are synchronously emulsified by the central oil channel; $Q_x = 60\ \mu L\,h^{-1}$, $Q_o = 650\ \mu L\,h^{-1}$, $Q_y = 120\ \mu L\,h^{-1}$. b) Fusion module. Paired droplets can be coalesced by applying an electrical voltage U between the two electrodes. c) Formation of iron oxide precipitates after coalescence of pairs of droplets. Reproduced from Ref. [100].

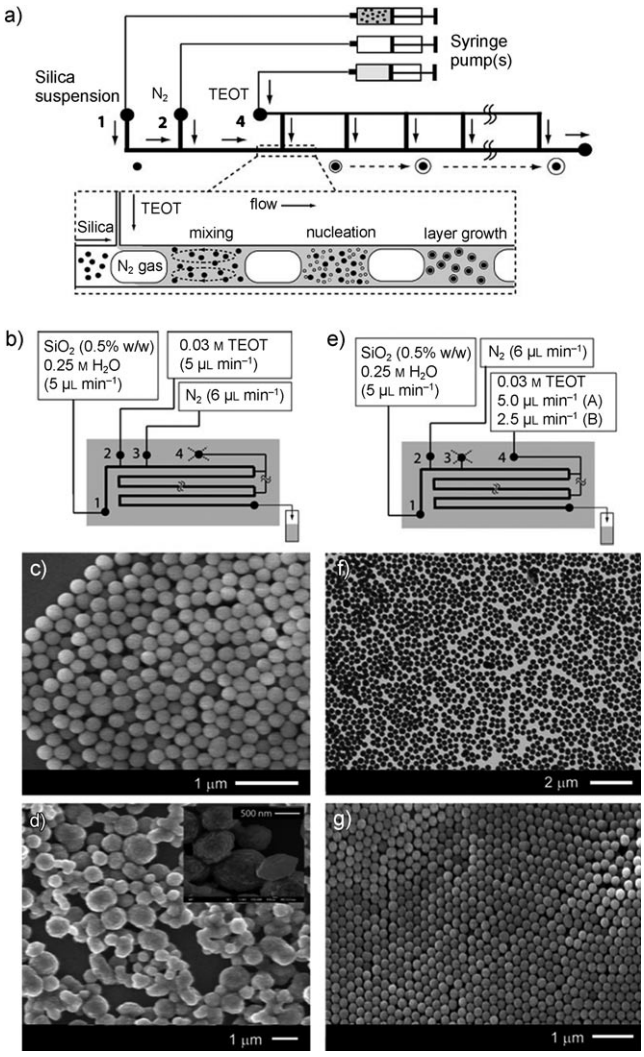

Figure 12. a) Design concept for a continuous-flow coating reactor. b) Details of the single-step titanium tetraethoxide (TEOT) addition experiments. The branched manifold was not used in this case. c) SEM of silica particles used for the coating experiments (average diameter = 209 nm, standard deviation (σ = 11 nm). d) SEM of particles obtained from the single-addition experiment. Inset shows a high magnification SEM of the particle surface. e) Details of the multistep TEOT addition experiments. The branched manifold was used in this case. f) Low-magnification TEM of coated particles. g) SEM of coated particles after calcination at 500 °C. Reproduced from Ref. [104].

the particles was evidenced by TEM images, which showed that the coating was composed of compact grains of titania deposited onto the primary silica surface. The microfluidic approach also allowed the tuning of the particle size by varying the addition rate of TEOT.

We also reported the multistep continuous-flow synthesis of magnetic and fluorescent core/shell γ-Fe_2O_3/SiO_2 nanoparticles by using several flow-focusing microreactors (Figure 13).[87] Three microreactors were connected in series, each one acting as a micro-unit for a defined operation. The first microreactor enabled the grafting of (3-aminopropyl) triethoxysilane (APTES) on the surface of γ-Fe_2O_3 nanoparticles previously coated by citrate ligands. The second microreactor enabled the fast mixing of the modified magnetic nanoparticles with the fluorescent silica shell precursors TEOS and APTES labeled with the fluorescent dye rhodamine B isothiocynanate. The final microreactor served for the hydrolysis–condensation reaction of the silica precursors catalyzed by NH_3 onto the magnetic nanoparticles. TEM images confirmed the acceleration of the coating process, as core/shell structures were observed after only 7 min compared to several hours in a conventional bath process. Furthermore, fluorescent chain-like structures were observed by fluorescence microscopy in the presence of a magnetic field, thereby providing evidence for the bifunctional character of the nanoparticles (Figure 13c).

4.4. Synthesis of Metallic Nanoparticles

The optical, electronic, and thermal properties of metallic nanoparticles endow them with potential applications in electrical and nonlinear optical devices,[105] improved dielectric materials,[106] nanomaterials for bioimaging or hyperthermia,[107] and high thermal conductivity nanofluids.[108] Synthesis of Au,[109–114] Ag,[32,115] Cu,[116] and Pd[117] nano-

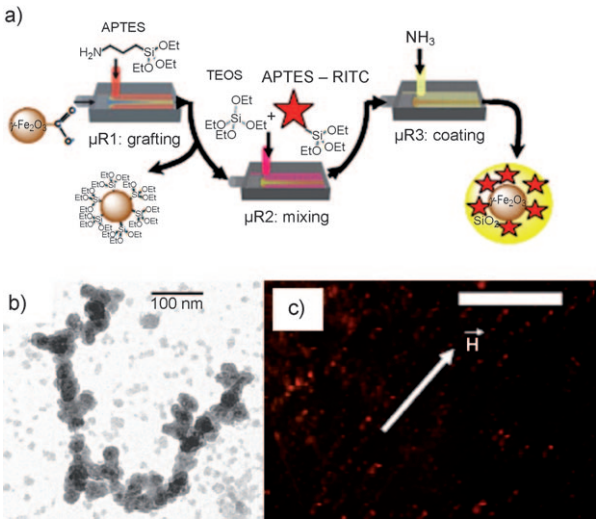

Figure 13. a) Illustration of the coaxial-flow microreactor (μR) showing the mixing between the inner stream (Q_{in}) and the outer stream (Q_{out}) for the continuous synthesis of fluorescent core/shell MNPs/silica nanoparticles. μR1 = microreactor for APTES grafting on the citrated γ-Fe_2O_3 nanoparticles; μR2 = microreactor for mixing of the sol–gel precursors TEOS and APTES-RITC; μR3 = microreactor for coating of the γ-Fe_2O_3 nanoparticles with silica. MNPs = magnetic nanoparticles, APTES = (3-aminopropyl)triethoxysilane, TEOS = tetraethyl orthosilicate, RITC = rhodamine B isothiocyanate. b) TEM micrographs showing typical architectures of the core/shell MNPS@SiO_2(RITC) nanoparticles. c) Fluorescence microscopy images of silica-coated iron oxide nanoparticles in the presence of an external magnetic field showing the formation of chain-like structures. Scale bar: 50 μm. Reproduced from Ref. [87].

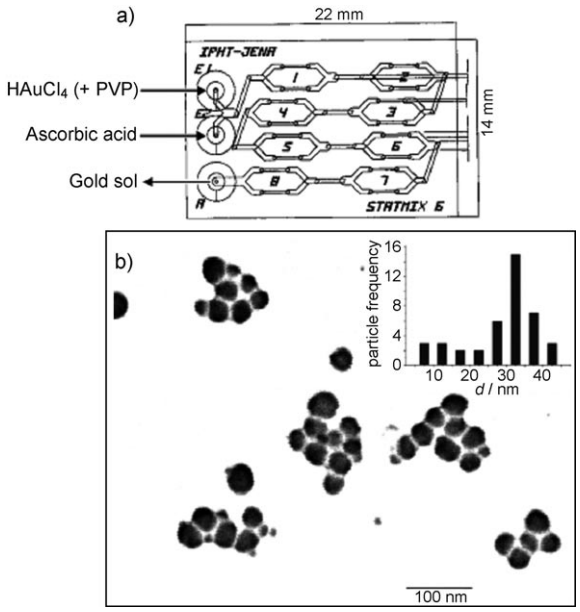

Figure 14. a) The experimental setup of the IPHT microreactor showing the connectivity (STATMIX 6, area 22×14 mm). b) SEM image (with particle size analysis as inset) of gold particles obtained at a flow rate of 500 μL min^{-1} (native reactor, pH 2.8, 1 mM $HAuCl_4$, 20 mM ascorbic acid, 0.025% PVP). Reproduced from Ref. [110], copyright American Chemical Society 2005.

particles in microfluidic reactors have been reported. Owing to their greatly enhanced light absorption (Mie scattering) at the plasmon resonance wavelength,[118–120] the growth and shape of metallic nanoparticles can be monitored optically, thus offering a convenient system to be studied in microfluidic devices.

Wagner et al. reported the synthesis of 15 to 24 nm spherical gold nanoparticles, at room temperature, in a chip-based diffusion microreactor following a seeding growth approach.[109] To initiate the growth of larger gold nanoparticles, the microsynthesis started from 12 nm citrate-stabilized gold seeds, which were conventionally synthesized out the microsystem. Ascorbic acid was used as a soft reducing agent of $HAuCl_4$ at the surface of the 12 nm seeds, serving as nuclei of the final particles, the latter being stabilized against aggregation by polyvinyl pyrrolidone (PVP). Off-line techniques (analytical centrifugation and AFM) enabled a mean particle diameter to be deduced, which was larger when the flow rate decreased. Later, the same authors used a continuous-flow microreactor for the synthesis of gold nanoparticles (5 to 50 nm) by reducing the gold precursor $HAuCl_4$ by ascorbic acid in the presence of PVP (Figure 14).[110] Several parameters, such as the flow rate, pH, reagent concentrations, and PVP concentration were screened. Surface modification of the microsystem to avoid fouling and adsorption of the nanoparticles onto the microreactor walls was also examined. This microfluidic device produced gold nanoparticles with a size distribution width twice as narrow as that obtained in a conventional synthesis.

To obtain very small gold nanoparticles, the same authors used borohydride $NaBH_4$ as a stronger reducing agent during the synthesis in the microfluidic reactor.[113] This reducing agent and the same microreactor were also used for the synthesis of silver nanoparticles from $AgNO_3$ precursor, followed by a direct surface modification with thiol ligands. The direct reduction of $HAuCl_4$ with $NaBH_4$ reproducibly produced gold nanoparticles with a diameter ranging between 4 and 7 nm. In the investigated flow-rate range, no variation of the particle size distribution was observed when the flow rate was varied. The same behavior was observed when the concentration ratio of the precursor to the reducing agent and the pH was varied. The mean diameters of corresponding silver nanoparticles were much larger (ca. 15 nm). Even though the mean particles size of the silver nanoparticles was as little affected by the flow rate as for gold, the size distribution width was lowered by either increasing the flow rate or increasing the $NaBH_4/AgNO_3$ ratio, in contrast to what was observed for gold nanoparticles. The same group also reported on the synthesis in microreactors of bimetallic nanoparticles with various compositions of silver and gold for catalytic applications. They showed that the optical properties of the colloidal product solutions were affected by the mixing order of the reactant solutions and the overall flow rates.

Microfluidic continuous-flow synthesis of rod-shaped gold and silver nanocrystals was described by Boleininger et al.[112] They adapted the synthesis method originally described by Nikoobakht et al.[121] and Jana et al.[119] to a microfluidic

process. Conventionally, the method is based on the growth of metal nanorods from spherical metal seed crystals in an aqueous growth solution containing the $HAuCl_4$ or $AgNO_3$ precursors, a soft reducing agent, such as ascorbic acid, and a high concentration of a surfactant molecule, such as cetyltrimethylammonium bromide (CTAB) surfactant. The microreactors used in this study consisted of a PVC capillary tube (1 mm id) for the gold nanorod synthesis and a polyetheretherketone (PEEK) tube (0.75 mm id) for the silver nanorod synthesis; both were immersed in a heat bath maintained at 30 °C. The UV/Vis spectra (optical extinction) of the final product were measured at the outlet of the reactor by a flow-through spectrometer to approximate the aspect ratio of the nanorods. The effect of the ratio *r* of growth to seed solution and of temperature on the final particles was investigated.

Thermal reduction of silver pentafluoropropionate in the presence of trioctylamine (TOA) as a surfactant in isoamyl ether was reported by Lin et al. as a method for the synthesis of silver nanoparticles in a continuous-flow tubular microreactor.[115] Unlike the commonly used methods for producing silver nanoparticles from silver salts in aqueous solution, the thermal reduction method described by the authors was a single-phase system that is suitable to generate narrow size dispersions. The synthesis mixture was introduced into a tubular coil made of a stainless-steel needle (0.84 mm id) heated to a temperature of between 100 and 140 °C using an oil bath (Figure 15). The ratio TOA/silver pentafluoropropionate, the flow rate, the temperature versus time profiles, and the reaction temperature of the reactor were varied to investigate their effects on the average size and distribution range of the silver nanoparticles. Oleylamine was used as a capping agent to stabilize the nanoparticles at the outlet of the reactor before they were analyzed by TEM and off-line UV/Vis spectra. The change in the TOA concentration did not induce any substantial difference in either the size or size distribution of the nanoparticles, while an increase of diameters of the nanoparticles and of their polydispersity was observed when the flow rate was increased. He et al.[159] further studied the effect of the nature of the capillary tube on the synthesis of silver nanoparticles. Their results indicated that a high affinity between the particles and the interior wall of the tube resulted into a broader size distribution and a lower production yield. Another method based on the principle that a metal ion M^{n+} or complex ion can be reduced to its atomic state M^0 by another metal with a lower redox potential was reported by Wu et al. for the synthesis of Ag nanoparticles.[122] The authors used different metal foils (Ni, Fe, and Co) as heterogeneous reducing media and reactors to reduce $AgNO_3$ into silver colloids. The particle size and size distribution could be tuned depending on the metal foil and on the residence time. Fine silver halide nanoparticle synthesis AgX (X = Cl or Br) in an annular multi-lamination microreactor was reported by Nagasawa and Mae.[123] They successfully achieved a stable and continuous synthesis without any clogging of the microchannel by flowing inactive fluids in the outermost and innermost annular streams. The influence of different operational parameters on the volume flow rates of the inactive fluids and the flowing solution in the middle stream on the particle size was investigated.

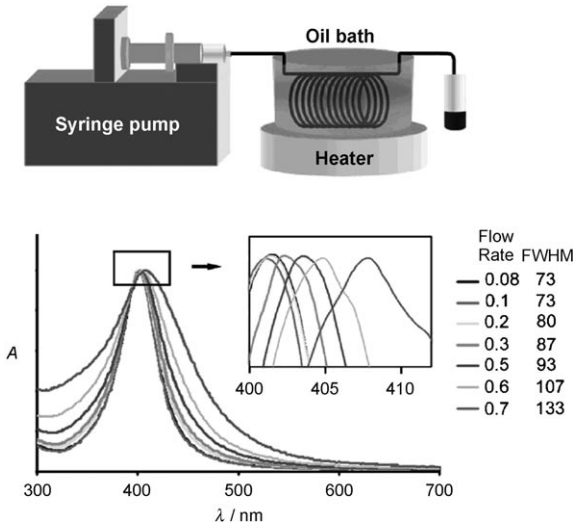

Figure 15. a) Experimental setup of the synthesis of silver nanoparticles in a tubular microreactor. b) UV/Vis absorption spectra of silver nanoparticles formed at different flow rates. Insets show the enlarged peak region and a summary of FWHMs of the absorbance [nm] of the silver nanoparticles at the various volumetric flow rates [mL min^{-1}] used. Reproduced from Ref. [115], copyright American Chemical Society 2004.

The synthesis of size-controlled palladium nanoparticles was evidenced by Song et al. using a polymer-based microfluidic reactor.[117] The polymeric continuous-flow microreactor was fabricated using a negative photo resist SU-8 on a 10 × 10 cm^2 PEEK substrate by standard UV photolithography. The palladium nanoparticles were synthesized by reduction of $PdCl_2$ by $LiBEt_3H$ in THF. The nanoparticles were characterized by TEM, selected-area electron-diffraction (SAED), and X-ray diffraction. The palladium nanoparticles synthesized in the microreactor were found to have a narrower size distribution compared with those obtained by a conventional batch process. The same authors also reported on the synthesis of copper nanoparticles.[116] Compared with those produced by the conventional batch process, the copper nanoparticles formed in microfluidic devices were smaller (8.9 nm vs. 22.5 nm) and had a narrower size distribution and an improved stability versus oxidation. Cobalt nanoparticles were synthesized in a microfluidic reactor with three different crystal structures—face-centered cubic (fcc), hexagonal closest-packed (hcp) and ε-cobalt—according to the reaction times, flow rates, and quenching procedures.[47] Zinoveva et al. probed the cobalt nanoparticle formation at three different positions in a poly(methyl methacrylate) (PMMA) microreactor using synchrotron-radiation-based X-ray absorption spectroscopy.[124] Co-K edge XANES spectra recorded at three different positions of the microchannel together with reference spectra of the precursor and the final product collected at the end of microfluidic system showed that a time resolution of the reaction of the order of milliseconds can be obtained from the spatial resolution within the microreactor, thus showing the power of the position–time equivalency in continuous-flow microfluidics.

4.5. Microfluidics for Advanced Materials Science

As described above, the confinement and mass transport phenomena associated with microfluidics are well-suited for the controlled synthesis and modification of inorganic nanoparticles. Microfluidic environments are also extremely promising for the controlled aggregation or encapsulation of inorganic nanoparticles to produce higher-order, typically microscopic structures with multifunctional properties.

4.5.1. Self-Assembly of Colloids

Three-dimensional assemblies of monodisperse colloids have received much attention, primarily because of their potential as optical materials, for example as photonic crystals.[125,126] Similar to semiconductors in electronic devices, these photonic crystals can exhibit optical insulating behavior due to a photonic bandgap (PBG).[127,128] The controlled preparation of colloidal photonic crystals is challenging, as the process is usually governed by self-organization.[129] Materials with three-dimensional structures ordered over multiple length scales can be prepared by carrying out colloidal crystallization and inorganic/organic self-assembly within microfluidic channels.[130]

Whitesides and co-workers reported the first result on polymeric colloidal crystallization inside PDMS channels.[131] Later, the same group created inverted opaline structures with inorganic titania sol by infiltrating a titania precursor into the interstices of opaline structure and subsequently removing the particles.[130] A facile route for the fabrication of cylindrical colloidal crystals (CylCCs) by self-assembly inside a microcapillary (Figure 16) was reported by Moon et al.[132] Furthermore, inorganic inverted replicas of the CylCCs were prepared by using the shaped colloidal crystals as templates. Inorganic CylCCs were obtained by using different types of particles and microcapillaries.

A droplet-based microfluidic device was also used to create self-assemblies of colloidal particles. Kim et al. encapsulated silica colloidal particles in aqueous emulsion droplets generated in an oil phase by using a co-flowing stream.[133] The controlled microwave irradiation of the aqueous drop led to the evaporation of the solvent and induced the self-organization of silica colloids into opaline photonic balls. Compared to conventional methods, the microwave-assisted evaporation reduced the time of evaporation and the consolidation of the colloidal particles. By controlling the microwave intensity, it was also possible to control the water evaporation rate. Inorganic photonic crystals with a good packing quality were obtained, and these showed photonic band-gap characteristics.

In-situ crystallization of colloidal particles in microfluidic chips (Figure 17) under a centrifugal force field was described in the work of Lee et al.[134] The colloidal crystallization proceeded much faster than conventional evaporation-induced crystallization. Although the processing time was dramatically reduced, the crystallinity was not seriously affected because the time scale of particle movement was still larger than the crystallization timescale. The sedimentation rate was proportional to the density difference that could be controlled by changing the dispersing media.

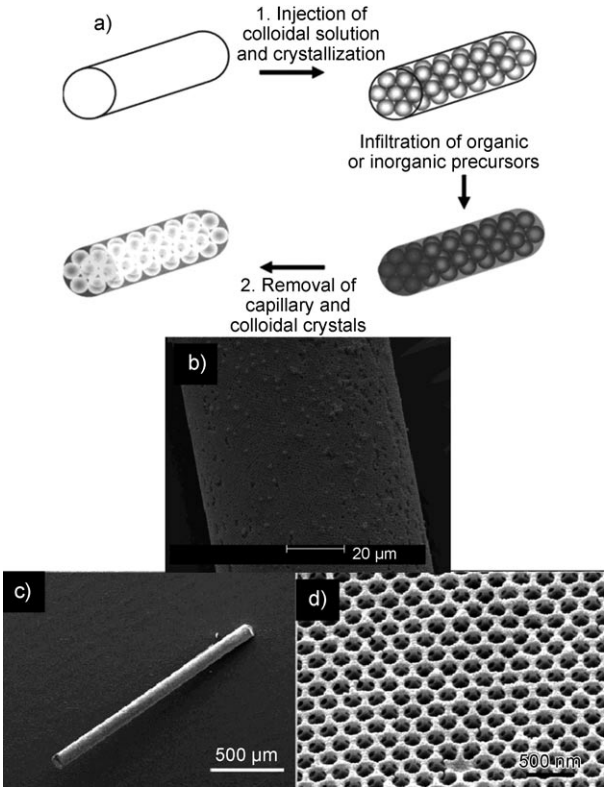

Figure 16. a) Diagram showing the fabrication of CylCC (1) and inverted structures from the CylCC template (2). b) SEM image of a CylCC of silica particles. The ratio of capillary to particle diameter is 65 μm/0.7 μm. c) SEM image of an ordered macroporous cylinder of silica substrate, and d) surface morphology. PS beads of 0.25 μm in diameter and a PMMA capillary of 125 μm in diameter were used for the colloidal crystal template. Reproduced from Ref. [132], copyright American Chemical Society 2004.

4.5.2. Controlled Aggregation of Metal Nanoparticles

The preparation of isolated and clustered gold nanoparticles at room temperature in the presence of polyelectrolyte molecules using a flow-through silicon chip reactor has been reported.[111] Ascorbic acid and iron(II) were used as reducing agents, and sodium metasilicate and poly(vinyl alcohol) were added as effectors for the formation of the nanoparticles. The successive addition of reaction components in the micro-continuous-flow process was tested. Single particles of different sizes, simple particles aggregates, core/shell particles, and also complex aggregates and hexagonal nanocrystallites were obtained according to the experimental conditions. Tsunoyoma and co-workers successfully prepared small PVP-stabilized gold clusters by an homogeneous mixing of continuous flows of aqueous $AuCl_4^-$ and BH_4^- in a micromixer (Figure 18).[135] With this method, small Au:PVP nanoparticles with a higher catalytic activity than clusters produced by conventional batch methods were prepared.

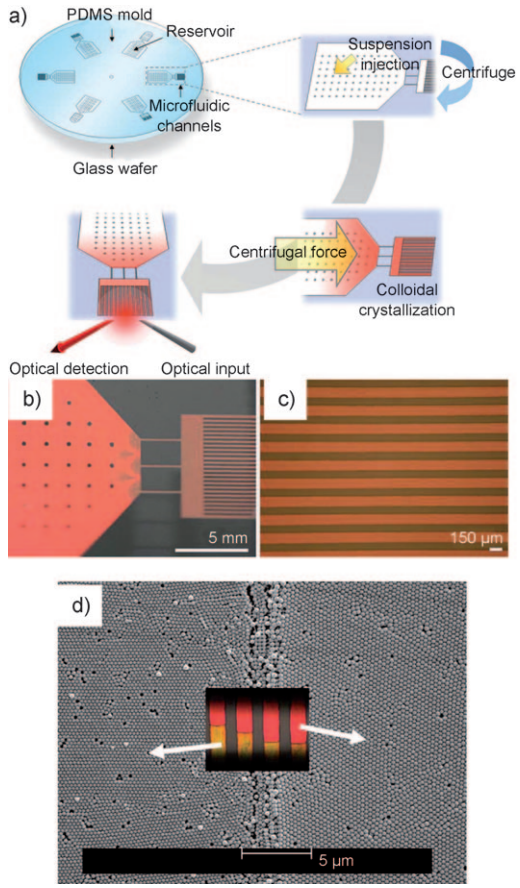

Figure 17. a) Arrangement of designed functional units of the centrifugal microfluidic chip and procedure for crystallization of colloidal particles in a centrifugal microfluidic platform. Completely crystallized silica spheres 300 nm in diameter that reflect red light after centrifugation. b) Top view of a fluidic cell that has a set of parallel microchannels, c) colloidal crystal strips of silica spheres in microchannels. d) SEM image showing the interface of hybrid colloidal crystals composed of 255 nm and 300 nm silica particles. In the inset, the optical microscope image displays different reflection colors from two constituting parts of the hybrid colloidal crystals. Reproduced from Ref. [134], copyright the Royal Society of Chemistry 2006.

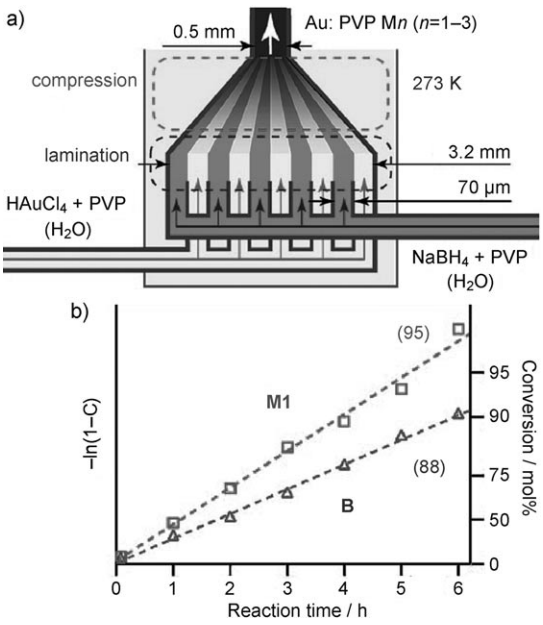

Figure 18. a) Synthesis of PVP-stabilized gold clusters in a micromixer. M is the sample mane and *n* is the number of the sample (1–3). b) Time course of the yield of the product *p*-hydroxybenzaldehyde. The numbers in parentheses indicate the isolated yields after the reactions had been conducted for 6 h. M1 is Au:PVP prepared in microfluidic reactor, and B is Au:PVP prepared by the conventional batch method. Reproduced from Ref. [135], copyright American Chemical Society 2008.

4.5.3. *Colloids Based on Inorganic Materials*

Chang et al. encapsulated CdSe/ZnS QDs into uniform-sized microcapsules made of a biocompatible copolymer, poly(D,L-lactide-*co*-glycolide) (PLGA), utilizing a microfluidic chip.[136] A blend of poly(vinyl alcohol) (PVA) and chitosan (CS) as stabilizers was formulated to produce the hydrophobic PLGA polymer matrix entrapping CdSe/ZnS Qds. The PLGA polymer solution was constrained to adopt the spherical droplets geometry by flowing into a continuous aqueous phase at a microchannel T cross-junction. By adjusting the flow conditions of the two immiscible solutions, PLGA microgels encapsulating CdSe/ZnS QDs were produced with diameters ranging form 180 to 550 μm. In contrast to individual QDs, the PLGA microsphere, which encapsulates thousands of Qds, presented a highly amplified and reproducible signal for fluorescence-based bioanalysis.

The encapsulation of polystyrene-stabilized CdS quantum dots (PS-CdS) into mesoscale aqueous spherical assemblies, named quantum-dot compound micelles (QDCMs) was performed using either a single-phase flow-focusing reactor or a two-phase gas–liquid-segmented microfluidic reactor.[137,138] Self-assembly was initiated by the addition of water to a blended solution of PS-coated CdS nanoparticles and amphiphilic polystyrene-*block*-poly(acrylic acid) copolymer stabilizing chains (PS-*b*-PAA). In the single-phase flow-focusing regime, the QDCM formation was initiated in a central stream by cross-stream diffusion of water from a surrounding sheath stream followed by a downstream quench step. In this case, on-chip size control was exerted either by the steady-state water concentration or the flow rate. However, QDCM polydispersities from this microfluidic approach were comparable to those obtained in the bulk (ca. 30% relative standard deviations). This was partially attributed to the limitations of diffusion controlled mixing and to the large residence-time distributions that are characteristic of single-phase reactors.

In the segmented-flow approach, QD association was initiated by the fast mixing of the reagents by chaotic advection within liquid plugs moving through a sinusoidal channel. Subsequent recirculating flow within a post-formation channel subjected the dynamic QDCMs to shear-induced processing, which was controlled by the flow rate and channel length, before a final quench into pure water. It appeared that enhanced mixing alone was insufficient to explain the improvement in the QDCM polydispersities, and that the

mean sizes and the polydispersity of the assemblies immediately following association was largely governed by the steady-state water content, regardless of the very different mixing times. However, mean QDCM sizes and polydispersities were both significantly decreased in the post-formation channel by tuning the self-assembly process, which was attributed to shear-induced particle breakup within the internal back-flow fields of the liquid plugs.

Monodisperse multifunctional and mesoporous inorganic microspheres with a worm-like disordered pore structure were generated using microfluidic devices by forming uniform droplets of an aqueous-based precursor solution in a T-shaped microfluidic device followed by ex-situ evaporation-induced self-assembly in a batch reactor.[139] The procedure was tuned to produce well-separated particles or alternatively particles that were linked together. To benefit from the full potential of a microfluidic-based particle generation, Lee and co-workers described a one-step in-situ method named microfluidic diffusion-induced self-assembly for the synthesis of monodisperse and ordered mesoporous silica microspheres (Figure 19).[140] The method combines microfluidic generation of uniform droplets of ethanol-rich precursor phase and subsequent in-situ rapid solvent-diffusion-induced self-assembly within the microfluidic channel. Well-ordered two-dimensional hexagonal mesostructures with an unprecedented corrugated surface morphology of disordered mesopores larger than 15 nm were prepared by this method. The surface morphology and the particle size of the mesoporous silica microspheres were systematically controlled by adjusting the microfluidic conditions.

In-situ preparation of monodisperse hybrid Janus microspheres (HJMs) with inorganic allyl hydrido polycarbosilane and organic perfluoropolyether constituents was demonstrated by using a hydrodynamic flow-focusing device.[141] A photocurable oligomer solution was generated into an immiscible continuous phase. The size and shape of the HJMs was controlled by varying the flow rate of the oligomer solution and of the continuous phase. The selective incorporation of magnetic Fe_3O_4 into the inorganic allylhydridopolycarbosilane lobe of the HJM was performed to produce microspheres displaying a magnetic-field-induced behavior.

Single-step fabrication of TiO_2 microspheres with embedded functional CdS and Fe_2O_3 nanoparticles were also fabricated in a three-dimensional co-flow microfluidic device.[142] The functional nanoparticles were confined mainly in the titania shells of the resulting hollow spheres, which were highly monodisperse and with a good stability against coagulation.

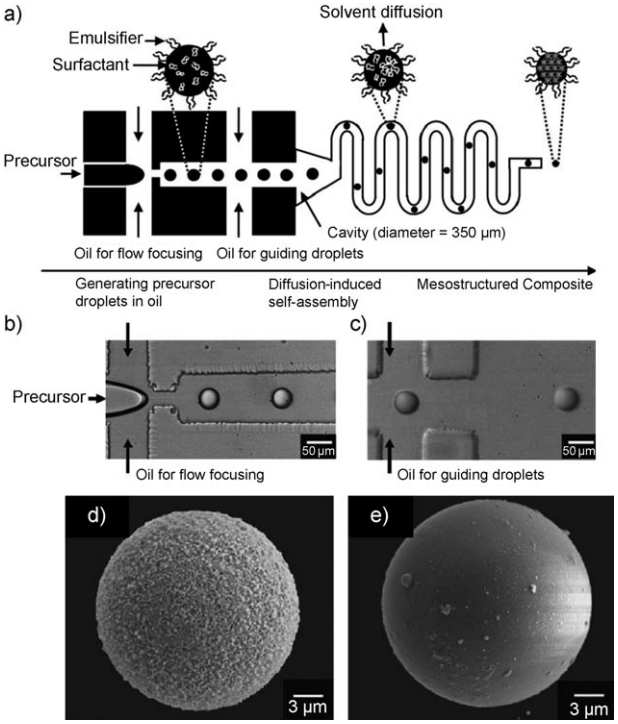

Figure 19. a) Illustration of the synthesis of ordered mesoporous silica particles using microfluidic diffusion-induced self-assembly (DISA). Monodisperse droplets are generated at the T-shaped flow-focusing orifice and assembled into mesostructured silica/surfactant composite spheres by rapid DISA in situ within the microchannel. b,c) Optical micrographs of b) the T-shaped flow-focusing orifice generating droplets at the orifice, and c) the T junction that guides flow to prevent droplet collision by increasing interdroplet distance. d,e) Control of the surface morphology of mesoporous silica microspheres: SEM images of mesoporous silica spheres generated in d) hexadecane and e) mineral oil. Reproduced from Ref. [140].

5. Conclusions and Outlook

This Review aimed to cover different aspects of microfluidics in the field of inorganic chemistry. The high area/volume ratios and the significantly reduced diffusion distance in microfluidic systems are the most commonly known advantages that are attractive enough to convince researchers to adapt their chemical applications of interest at a microfluidic scale. In the field of inorganic extraction, innovative work has been done, but these were limited to the simple separation of a few metallic species. The microfluidic synthesis of inorganic or bioinorganic molecular compounds or clusters in their discrete or crystalline forms also remains poorly explored. In the field of inorganic chemistry, microfluidic processes until now have mainly focused on the optimization of nanomaterials synthesis. Compared to conventional methods, the physical properties were improved and better control of the size and of the polydispersity of particles was possible.

Quantum dots are an area of great interest, which is probably due to the ease of using on-line characterization methods (absorption and fluorescence spectroscopy) to study their synthesis process. Fluorescence has been mostly used because of its simplicity of implementation in microscopic formats and its widespread use as a sensitive and quantitative spectroscopic tool. Nevertheless, most inorganic materials are not fluorescent, and characterization has to be completed by using off-line analytical methods, such as X-ray spectroscopy or transmission electron microscopy. On-line integration of analysis within the microchemical systems would allow a better optimization and access to the kinetic parameters of the chemical reactions. Integration and development of analytical methods, such as electrophoresis,[66] NMR spec-

troscopy,[143–145] mass spectrometry,[146] and FTIR,[147] IR,[148] and Raman spectroscopy,[149–151] that are devoted to kinetic studies of organic reactions have been described. However, in the field of inorganic materials chemistry, UV/Vis spectroscopy appears to be the only available in-situ method.

Very recently, a free-jet micromixer was coupled to small angle X-ray scattering (SAXS) on a synchrotron beamline to acquire kinetic data on the nucleation and growth of nanoparticles.[152] It is a very powerful technique but it cannot be coupled so easily to microfluidic devices. This difficulty to find a convenient technique to ensure an on-line characterization of nanoparticles is an important limitation to achieve the optimization of inorganic synthesis in microreactors, and development of on-line characterization methods must be the priority in the next few years.

Addendum (January 29, 2010)

Performing inorganic chemical reactions in microchannels has been increasingly more established as a method for the preparation of inorganic nanomaterials. During the time since submission of this Review, new research has been published in the field of inorganic chemistry using microfluidics. These publications cover new techniques and devices for the comprehension of fundamental aspects of this chemistry, such as the nucleation and growth of nanoparticles,[153] the synthesis of metallic nanoparticles with different shapes,[154] quantum dots, and oxide nanoparticles.[155–158]

Received: July 31, 2009
Revised: February 1, 2010
Published online: August 2, 2010

[1] A. Manz, N. Graber, H. M. Widmer, *Sens. Actuators B* **1990**, *1*, 244 – 248.
[2] A. Manz, D. J. Harrison, E. Verpoorte, J. C. Fettinger, H. Lundi, M. Widmer, *Chimia* **1991**, *45*, 103 – 105.
[3] A. Manz, D. J. Harrison, E. Verpoorte, M. Widmer, *Adv. Chromatogr.* **1993**, *33*, 1.
[4] A. Van den Berg, T. S. J. Lammerink, *Top. Curr. Chem.* **1998**, *194*, 21.
[5] P. S. Dittrich, A. Manz, *Nat. Rev. Drug Discovery* **2006**, *5*, 210 – 218.
[6] J. M. Ramsey, S. C. Jacobson, M. R. Knapp, *Nat. Med.* **1995**, *1*, 1093 – 1095.
[7] S. J. Haswell, P. Watts, *Green Chem.* **2003**, *5*, 240 – 249.
[8] J.-i. Yoshida, A. Nagaki, T. Yamada, *Chem. Eur. J.* **2008**, *14*, 7450 – 7459.
[9] D. Belder, *Angew. Chem.* **2009**, *121*, 3790 – 3791; *Angew. Chem. Int. Ed.* **2009**, *48*, 3736 – 3737.
[10] a) W. Ehrfeld, V. Hessel, H. Löwe, *Microreactors: New Technology for Modern Chemistry*, Wiley-VCH, Weinheim, **2000**; b) V. Hessel, H. Löwe, A. Müller, G. Kolb, *Chemical Micro Process Engineering. Fundamentals, Modelling and Reactions/Processes and Plants*, Wiley-VCH, Weinheim, **2005**; c) N. Kockmann, O. Brand, G. K. Fedder, *Micro Process Engineering*, Wiley-VCH, Weinheim, **2006**; d) J. Yoshida, *Flash Chemistry. Fast Organic Synthesis in Microsystems*, Wiley-Blackwell, **2008**; e) *Micro Process Engineering, A Comprehensive Handbook* (Eds.: V. Hessel, J. C. Schouten, A. Renken, J. Yoshida), Wiley, Hoboken, **2009**.
[11] G. M. Whitesides, *Nature* **2006**, *442*, 368 – 373.
[12] J. West, M. Becker, S. Tombrink, A. Manz, *Anal. Chem.* **2008**, *80*, 4403 – 4419.
[13] D. Psaltis, S. R. Quake, C. Yang, *Nature* **2006**, *442*, 368 – 373.
[14] A. J. deMello, *Nature* **2006**, *442*, 394 – 402.
[15] M. Joanicot, A. Ajdari, *Science* **2005**, *309*, 887 – 888.
[16] D. M. Ratner, E. R. Murphy, M. Jhunjhunwala, D. A. Snyder, K. F. Jensen, P. H. Seeberger, *Chem. Commun.* **2005**, 578 – 580.
[17] R. D. Chambers, M. A. Fox, D. Holling, T. Nakano, T. Okazoe, G. Sandford, *Lab Chip* **2005**, *5*, 191 – 198.
[18] J. Knight, *Nature* **2002**, *418*, 474 – 475.
[19] J. Hogan, *Nature* **2006**, *442*, 351 – 352.
[20] H. A. Stone, A. D. Stroock, A. Ajdari, *Annu. Rev. Fluid Mech.* **2004**, *36*, 381 – 411.
[21] T. M. Squires, S. R. Quake, *Rev.Mod. Phys.* **2005**, *77*, 977 – 1026.
[22] K. Jähnisch, V. Hessel, H. Löwe, M. Baerns, *Angew. Chem.* **2004**, *116*, 410 – 451; *Angew. Chem. Int. Ed.* **2004**, *43*, 406 – 446.
[23] J. Kobayashi, Y. Mori, K. Okamoto, R. Akiyama, M. Ueno, T. Kitamori, S. Kobayashi, *Science* **2004**, *304*, 1305 – 1308.
[24] C. L. Hansen, E. Skordalakes, J. M. Berger, S. R. Quake, *Proc. Natl. Acad. Sci. USA* **2002**, *99*, 16531 – 16536.
[25] J. Atencia, D. J. Beebe, *Nature* **2005**, *437*, 648 – 655.
[26] N.-T. Nguyen, Z. Wu, *J. Micromech. Microeng.* **2005**, *15*, R1 – R16.
[27] J. M. Ottino, S. Wiggins, *Philos. Trans. R. Soc. London Ser. A* **2004**, *362*, 923 – 935.
[28] H. Löwe, W. Ehrfeld, *Electrochim. Acta* **1999**, *44*, 3679 – 3689.
[29] P. Tabeling, *Introduction to microfluidics*, Oxford University Press, Oxford, **2005**.
[30] J. B. Knight, A. Vishwanath, J. P. Brody, R. H. Austin, *Phys. Rev. Lett.* **1998**, *80*, 3863 – 3866.
[31] H. Song, D. L. Chen, R. F. Ismagilov, *Angew. Chem.* **2003**, *115*, 792 – 796; *Angew. Chem. Int. Ed.* **2003**, *42*, 768 – 772.
[32] B. K. H. Yen, A. Günther, M. A. Schmidt, K. F. Jensen, M. G. Bawendi, *Angew. Chem.* **2005**, *117*, 5583 – 5587; *Angew. Chem. Int. Ed.* **2005**, *44*, 5447 – 5451.
[33] E. A. Mansur, M. Ye, Y. Wang, Y. Dai, *Chin. J. Chem. Eng.* **2008**, *16*, 503 – 516.
[34] A. Günther, K. F. Jensen, *Lab Chip* **2006**, *6*, 1487 – 1503.
[35] J. M. Ottino, *Annu. Rev. Fluid Mech.* **1990**, *22*, 207 – 254.
[36] V. Hessel, H. Löwe, F. Schönfeld, *Chem. Eng. Sci.* **2005**, *60*, 2479 – 2501.
[37] W. Ehrfeld, V. Hessel, H. Lowe, *Microreactors*, Wiley-VCH, Weinheim, **2000**.
[38] P. Gravesen, J. Branjeberg, O. S. Jensen in *Micro Mechanics Europe, MME'93*, Neuchatel, Switzerland, **1993**, p. 143.
[39] K. F. Jensen, *Chem. Eng. Sci.* **2001**, *56*, 293 – 303.
[40] C. Alépée, L. Vulpescu, P. Cousseau, P. Renaud, R. Maurer, A. Renken in *IMRET 4:4th International Conference on Microreaction Technology*, American Institute of Chemical Engineers Topical Conference Proceedings, Atlanta, USA, **2000**, p. 71.
[41] H. Pennemann, V. Hessel, H. Löwe, *Chem. Eng. Sci.* **2004**, *59*, 4789 – 4794.
[42] G. N. Doku, W. Verboom, D. N. Reinhoudt, A. van den Berg, *Tetrahedron* **2005**, *61*, 2733 – 2742.
[43] H. R. Sahoo, J. G. Kralj, K. F. Jensen, *Angew. Chem.* **2007**, *119*, 5806 – 5810; *Angew. Chem. Int. Ed.* **2007**, *46*, 5704 – 5708.
[44] A. Abou-Hassan, O. Sandre, S. Neveu, V. Cabuil, *Angew. Chem.* **2009**, *121*, 2378 – 2381; *Angew. Chem. Int. Ed.* **2009**, *48*, 2342 – 2345.
[45] M. Tokeshi, T. Minagawa, K. Uchiyama, A. Hibara, K. Sato, H. Hisamoto, T. Kitamori, *Anal. Chem.* **2002**, *74*, 1565 – 1571.
[46] B. K. H. Yen, N. E. Stott, K. F. Jensen, M. G. Bawendi, *Adv. Mater.* **2003**, *15*, 1858 – 1862.
[47] H. Song, D. L. Chen, R. F. Ismagilov, *Angew. Chem.* **2006**, *118*, 7494 – 7516; *Angew. Chem. Int. Ed.* **2006**, *45*, 7336 – 7356.

[48] H. Hotokezaka, M. Tokeshi, M. Harada, T. Kitamori, Y. Ikeda, *Prog. Nucl. Energy* **2005**, *47*, 439 – 447.
[49] M. Tokeshi, T. Kitamori, *Prog. Nucl. Energy* **2005**, *47*, 434 – 438.
[50] K. Sato, M. Tokeshi, T. Sawada, T. Kitamori, *Anal. Sci.* **2000**, *16*, 455 – 456.
[51] M. Tokeshi, M. Uchida, A. Hibara, T. Sawada, T. Kitamori, *Anal. Chem.* **2001**, *73*, 2112 – 2116.
[52] H.-B. Kim, K. Ueno, M. Chiba, O. Kogi, N. Kitamura, *Anal. Sci.* **2000**, *16*, 871 – 876.
[53] M. Tokeshi, T. Minagawa, T. Kitamori, *Anal. Chem.* **2000**, *72*, 1711 – 1714.
[54] T. Minagawa, M. Tokeshi, T. Kitamori, *Lab Chip* **2001**, *1*, 72 – 75.
[55] M. Tokeshi, T. Minagawa, T. Kitamori, *J. Chromatogr. A* **2000**, *894*, 19 – 23.
[56] T. Maruyama, T. Kaji, T. Ohkawa, K.-i. Sotowa, H. Matsushita, F. Kubota, N. Kamiya, K. Kusakabe, M. Goto, *Analyst* **2004**, *129*, 1008 – 1013.
[57] A. Hibara, M. Tokeshi, K. Uchiyama, H. Hisamoto, T. Kitamori, *Anal. Sci.* **2001**, *17*, 89 – 93.
[58] T. Maruyama, H. Matsushita, J.-i. Uchida, F. Kubota, N. Kamiya, M. Goto, *Anal. Chem.* **2004**, *76*, 4495 – 4500.
[59] H. Hisamoto, T. Horiuchi, K. Uchiyama, M. Tokeshi, A. Hibara, T. Kitamori, *Anal. Chem.* **2001**, *73*, 5551 – 5556.
[60] M. Kumemura, T. Korenaga, *Anal. Chim. Acta* **2006**, *558*, 75 – 79.
[61] H. Shen, Q. Fang, Z.-L. Fang, *Lab Chip* **2008**, *6*, 1387 – 1389.
[62] D. Kashchiev, *Nucleation Basic Theory with Applications*, Butterworth-Heinemann, Oxford, **2000**.
[63] K. F. Jensen, *MRS Bull.* **2006**, *31*, 101 – 107.
[64] Y. Song, J. Hormes, C. S. S. R. Kumar, *Small* **2008**, *4*, 698 – 711.
[65] Y. Xia, G. M. Whitesides, *Annu. Rev. Mater. Sci.* **1998**, *28*, 153 – 184.
[66] D. Belder, M. Ludwig, L.-W. Wang, M. T. Reetz, *Angew. Chem.* **2006**, *118*, 2523 – 2526; *Angew. Chem. Int. Ed.* **2006**, *45*, 2463 – 2466.
[67] A. J. deMello, J. C. deMello, *Lab Chip* **2004**, *4*, 11N – 15N.
[68] L.-H. Hung, A. P. Lee, *J. Med. Biol. Eng.* **2007**, *27*, 1 – 6.
[69] G. I. Taylor, *Proc. R. Soc. London Ser. A* **1953**, *219*, 186 – 203.
[70] P. Laval, A. Crombez, J.-B. Salmon, *Langmuir* **2009**, *25*, 1836 – 1841.
[71] J. B. Edel, R. Fortt, J. C. deMello, A. J. deMello, *Chem. Commun.* **2002**, 1136 – 1137.
[72] A. P. Alivisatos, *Science* **1996**, *271*, 933 – 937.
[73] M. A. Hines, P. Guyot-Sionnest, *J. Phys. Chem.* **1996**, *100*, 468 – 471.
[74] C. B. Murray, C. R. Kagan, M. G. Bawendi, *Annu. Rev. Mater. Sci.* **2000**, *30*, 545 – 610.
[75] C. D. Dushkin, S. Saita, K. Yoshie, Y. Yamaguchi, *Adv. Colloid Interface Sci.* **2000**, *88*, 37 – 78.
[76] E. M. Chan, R. A. Mathies, A. P. Alivisatos, *Nano. Lett.* **2003**, *3*, 199 – 201.
[77] F. G. Bessoth, A. J. deMello, A. Manz, *Anal. Commun.* **1999**, *36*, 213 – 215.
[78] I. Shestopalov, J. D. Tice, R. F. Ismagilov, *Lab Chip* **2004**, *4*, 316 – 321.
[79] L.-H. Hung, K. M. Choi, W.-Y. Tseng, Y.-C. Tan, K. J. Shea, A. P. Lee, *Lab Chip* **2006**, *6*, 174 – 178.
[80] T. L. Sounart, P. A. Safier, J. A. Voigt, J. Hoyt, D. R. Tallant, C. M. Matzke, T. A. Michalske, *Lab Chip* **2007**, *7*, 908 – 915.
[81] H. Nakamura, Y. Yamaguchi, M. Miyazaki, H. Maeda, M. Uehara, P. Mulvaney, *Chem. Commun.* **2002**, 2844 – 2845.
[82] S. Krishnadasan, J. Tovilla, R. Vilar, A. J. deMello, J. C. deMello, *J. Mater. Chem.* **2004**, *14*, 2655 – 2660.
[83] E. M. Chan, A. P. Alivisatos, R. A. Mathies, *J. Am. Chem. Soc.* **2005**, *127*, 13854 – 13861.
[84] S. Marre, J. Park, J. Rempel, J. Guan, M. G. Bawendi, K. F. Jensen, *Adv. Mater.* **2008**, *20*, 4830 – 4834.
[85] H. Yang, W. Luan, S.-t. Tu, Z. M. Wang, *Lab Chip* **2008**, *8*, 451 – 455.
[86] A. Singh, M. Limaye, S. Singh, L. Niranjan Prasad, C. K. Malek, S. Kulkarni, *Nanotechnology* **2008**, *19*, 245613.
[87] A. Abou-Hassan, R. Bazzi, V. Cabuil, *Angew. Chem.* **2009**, *121*, 7316 – 7319; *Angew. Chem. Int. Ed.* **2009**, *48*, 7180 – 7183.
[88] M. Bruchez, Jr., M. Moronne, P. Gin, S. Weiss, A. P. Alivisatos, *Science* **1998**, *281*, 2013 – 2016.
[89] B. O. Dabbousi, J. Rodriguez-Viejo, F. V. Mikulec, J. R. Heine, H. Mattoussi, R. Ober, K. F. Jensen, M. G. Bawendi, *J. Phys. Chem. B* **1997**, *101*, 9463 – 9475.
[90] H. Wang, X. Li, M. Uehara, Y. Yamaguchi, H. Nakamura, M. Miyazaki, H. Shimizu, H. Maeda, *Chem. Commun.* **2004**, 48 – 49.
[91] H. Wang, H. Nakamura, M. Uehara, Y. Yamaguchi, M. Miyazaki, H. Maeda, *Adv. Funct. Mater.* **2005**, *15*, 603 – 608.
[92] W. Luan, H. Yang, N. Fan, S.-T. Tu, *Nanoscale Res. Lett.* **2008**, *3*, 134 – 139.
[93] M. Uehara, H. Nakamura, H. Maeda in *World Congress on Medical Physics and Biomedical Engineering 2006*, **2007**, pp. 250–253.
[94] H. Wang, H. Nakamura, M. Uehara, M. Miyazaki, H. Maeda, *Chem. Commun.* **2002**, 1462 – 1463.
[95] M. Takagi, T. Maki, M. Miyahara, K. Mae, *Chem. Eng. J.* **2004**, *101*, 269 – 276.
[96] B. F. Cottam, S. Krishnadasan, A. J. DeMello, J. C. DeMello, M. S. P. Shaffer, *Lab Chip* **2007**, *7*, 167 – 169.
[97] H. Nagasawa, T. Tsujiuchi, T. Maki, K. Mae, *AIChE J.* **2007**, *53*, 196 – 206.
[98] S. A. Khan, A. Gunther, M. A. Schmidt, K. F. Jensen, *Langmuir* **2004**, *20*, 8604 – 8611.
[99] A. Abou Hassan, O. Sandre, V. Cabuil, P. Tabeling, *Chem. Commun.* **2008**, 1783 – 1785.
[100] L. Frenz, A. El Harrak, M. Pauly, S. Bégin-Colin, A. D. Griffiths, J.-C. Baret, *Angew. Chem.* **2008**, *120*, 6923 – 6926; *Angew. Chem. Int. Ed.* **2008**, *47*, 6817 – 6820.
[101] T. Miyake, T. Ueda, N. Ikenaga, H. Oda, M. Sano, *J. Mater. Sci.* **2005**, *40*, 5011 – 5013.
[102] W. Stöber, A. Fink, A. Bohn, *J. Colloid Interface Sci.* **1968**, *26*, 62 – 69.
[103] R. Massart, *IEEE Trans. Magn.* **1981**, *17*, 1247 – 1250.
[104] S. A. Khan, K. F. Jensen, *Adv. Mater.* **2007**, *19*, 2556 – 2560.
[105] F. Kim, J. H. Song, P. Yang, *J. Am. Chem. Soc.* **2002**, *124*, 14316 – 14317.
[106] K. Akamatsu, S. Deki, *J. Mater. Chem.* **1997**, *7*, 1773 – 1777.
[107] M. Kogiso, K. Yoshida, K. Yase, T. Shimizu, *Chem. Commun.* **2002**, 2492 – 2493.
[108] J. A. Eastman, S. U. S. Choi, S. Li, W. Yu, L. J. Thompson, *Appl. Phys. Lett.* **2001**, *78*, 718 – 720.
[109] J. Wagner, T. Kirner, G. Mayer, J. Albert, J. M. Köhler, *Chem. Eng. Sci.* **2004**, *101*, 251 – 260.
[110] J. Wagner, J. M. Köhler, *Nano Lett.* **2005**, *5*, 685 – 691.
[111] J. M. Köhler, J. Wagner, J. Albert, *J. Mater. Chem.* **2005**, *15*, 1924 – 1930.
[112] J. Boleininger, A. Kurz, V. Reuss, C. Sönnichsen, *Phys. Chem. Chem. Phys.* **2006**, *8*, 3824 – 3827.
[113] J. Wagner, T. R. Tshikhudo, J. M. Köhler, *Chem. Eng. J.* **2008**, *135*, S104 – S109.
[114] J. M. Köhler, L. Abahmane, J. Wagner, J. Albert, G. Mayer, *Chem. Eng. Sci.* **2008**, *63*, 5048 – 5055.
[115] X. Z. Lin, A. D. Terepka, H. Yang, *Nano Lett.* **2004**, *4*, 2227 – 2232.
[116] Y. Song, E. E. Doomes, J. Prindle, R. Tittsworth, J. Hormes, C. S. S. R. Kumar, *J. Phys. Chem. B* **2005**, *109*, 9330 – 9338.

[117] Y. Song, C. S. S. R. Kumar, J. Hormes, *J. Nanosci. Nanotechnol.* **2004**, *4*, 788 – 793.
[118] P. Mulvaney, *Langmuir* **1996**, *12*, 788 – 800.
[119] N. R. Jana, L. Gearheart, C. J. Murphy, *Adv. Mater.* **2001**, *13*, 1389 – 1393.
[120] M.-L. Wu, D.-H. Chen, T.-C. Huang, *Chem. Mater.* **2001**, *13*, 599 – 606.
[121] B. Nikoobakht, M. A. El-Sayed, *Chem. Mater.* **2003**, *15*, 1957 – 1962.
[122] C. Wu, T. Zeng, *Chem. Mater.* **2007**, *19*, 123 – 125.
[123] H. Nagasawa, K. Mae, *Ind. Eng. Chem. Res.* **2006**, *45*, 2179 – 2186.
[124] S. Zinoveva, R. De Silva, R. D. Louis, P. Datta, C. S. S. R. Kumar, J. Goettert, J. Hormes, *Nucl. Instrum. Methods Phys. Res. Sect. A* **2007**, *582*, 239 – 241.
[125] A. van Blaaderen, R. Ruel, P. Wiltzius, *Nature* **1997**, *385*, 321 – 324.
[126] J.-Y. Shiu, C.-W. Kuo, P. Chen, *J. Am. Chem. Soc.* **2004**, *126*, 8096 – 8097.
[127] G.-R. Yi, S.-J. Jeon, T. Thorsen, V. N. Manoharan, S. R. Quake, D. J. Pine, S.-M. Yang, *Synth. Met.* **2003**, *139*, 803 – 806.
[128] J. H. Moon, G. R. Yi, S. M. Yang, D. J. Pine, S. B. Park, *Adv. Mater.* **2004**, *16*, 605 – 609.
[129] S.-K. Lee, S.-H. Kim, J.-H. Kang, S.-G. Park, W.-J. Jung, S.-H. Kim, G.-R. Yi, S.-M. Yang, *Microfluid. Nanofluid.* **2008**, *4*, 129 – 144.
[130] P. Yang, A. H. Rizvi, B. Messer, B. F. Chmelka, G. M. Whitesides, G. D. Stucky, *Adv. Mater.* **2001**, *13*, 427 – 431.
[131] E. Kim, Y. Xia, G. M. Whitesides, *Adv. Mater.* **1996**, *8*, 245 – 247.
[132] J. H. Moon, S. Kim, G.-R. Yi, Y.-H. Lee, S.-M. Yang, *Langmuir* **2004**, *20*, 2033 – 2035.
[133] S.-H. Kim, S. Y. Lee, G.-R. Yi, D. J. Pine, S.-M. Yang, *J. Am. Chem. Soc.* **2006**, *128*, 10897 – 10904.
[134] S.-K. Lee, G.-R. Yi, S.-M. Yang, *Lab Chip* **2006**, *6*, 1171 – 1177.
[135] H. Tsunoyama, N. Ichikuni, T. Tsukuda, *Langmuir* **2008**, *24*, 11327 – 11330.
[136] J.-Y. Chang, C.-H. Yang, K.-S. Huang, *Nanotechnology* **2007**, *18*, 305305.
[137] G. Schabas, H. Yusuf, M. G. Moffitt, D. Sinton, *Langmuir* **2008**, *24*, 637 – 643.
[138] G. Schabas, C.-W. Wang, A. Oskooei, H. Yusuf, M. G. Moffitt, D. Sinton, *Langmuir* **2008**, *24*, 10596 – 10603.
[139] N. J. Carroll, S. B. Rathod, E. Derbins, S. Mendez, D. A. Weitz, D. N. Petsev, *Langmuir* **2008**, *24*, 658 – 661.
[140] I. Lee, Y. Yoo, Z. Cheng, H.-K. Jeong, *Adv. Funct. Mater.* **2008**, *18*, 4014 – 4021.
[141] N. Prasad, J. Perumal, C.-H. Choi, C.-S. Lee, D.-P. Kim, *Adv. Funct. Mater.* **2009**, *19*, 1656 – 1662.
[142] T. H. Eun, S.-H. Kim, W.-J. Jeong, S.-J. Jeon, S.-H. Kim, S.-M. Yang, *Chem. Mater.* **2009**, *21*, 201 – 203.
[143] H. Wensink, F. Benito-Lopez, D. C. Hermes, W. Verboom, H. J. G. E. Gardeniers, D. N. Reinhoudt, A. van den Berg, *Lab Chip* **2005**, *5*, 280 – 284.
[144] J. Bart, A. J. Kolkman, A. J. Oosthoek-de Vries, K. Koch, P. J. Nieuwland, H. Janssen, J. van Bentum, K. A. M. Ampt, F. P. J. T. Rutjes, S. S. Wijmenga, H. Gardeniers, A. P. M. Kentgens, *J. Am. Chem. Soc.* **2009**, *131*, 5014 – 5015.
[145] L.-S. Bouchard, S. R. Burt, M. S. Anwar, K. V. Kovtunov, I. V. Koptyug, A. Pines, *Science* **2008**, *319*, 442 – 445.
[146] L. M. Fidalgo, G. Whyte, B. T. Ruotolo, J. L. P. Benesch, F. Stengel, C. Abell, C. V. Robinson, W. T. S. Huck, *Angew. Chem.* **2009**, *121*, 3719 – 3722; *Angew. Chem. Int. Ed.* **2009**, *48*, 3665 – 3668.
[147] R. Herzig-Marx, K. T. Queeney, R. J. Jackman, M. A. Schmidt, K. F. Jensen, *Anal. Chem.* **2004**, *76*, 6476 – 6483.
[148] T. M. Floyd, M. A. Schmidt, K. F. Jensen, *Ind. Eng. Chem. Res.* **2004**, *44*, 2351 – 2358.
[149] S.-A. Leung, R. F. Winkle, R. C. R. Wootton, A. J. deMello, *Analyst* **2005**, *130*, 46 – 51.
[150] D. Schäfer, J. A. Squier, J. van Maarseveen, D. Bonn, M. Bonn, M. Müller, *J. Am. Chem. Soc.* **2008**, *130*, 11592 – 11593.
[151] F. Sarrazin, J.-B. Salmon, D. Talaga, L. Servant, *Anal. Chem.* **2008**, *80*, 1689 – 1695.
[152] B. Marmiroli, G. Grenci, F. Cacho-Nerin, B. Sartori, E. Ferrari, P. Laggner, L. Businaro, H. Amenitsch, *Lab Chip* **2009**, *9*, 2063 – 2069.
[153] J. R. Polte, R. Erler, A. F. Thunemann, S. Sokolov, T. T. Ahner, K. Rademann, F. Emmerling, R. Kraehnert, *ACS Nano* **2010**, *4*, 1076 – 1082.
[154] D. Suhanya, A. K. Saif, *Small* **2009**, *5*, 2828 – 2834.
[155] A. M. Nightingale, J. C. deMello, *ChemPhysChem* **2009**, *10*, 2612 – 2614.
[156] W.-B. Lee, C.-H. Weng, F.-Y. Cheng, C.-S. Yeh, H.-Y. Lei, G.-B. Lee, *Biomed. Microdevices* **2009**, *11*, 161 – 171.
[157] K. Shiba, M. Ogawa, *Chem. Commun.* **2009**, 6851 – 6853.
[158] J. Wacker, V. K. Parashar, M. A. M. Gijs, *Procedia Chemistry* **2009**, *1*, 377 – 380.
[159] S. He, T. Kohira, M. Uehara, T. Kitamura, H. Nakamura, M. Miyazaki, H. Maeda, *Chem. Lett.* **2005**, *34*, 748 – 749.

